Available online at www.sciencedirect.com
SCIENCE DIRECT®
International Journal of Solids and Structures 42 (2005) 1009–1038
INTERNATIONAL JOURNAL OF SOLIDS and STRUCTURES
www.elsevier.com/locate/ijsolstr

A two-dimensional, higher-order, elasticity-based micromechanics model

Todd O. Williams *

Theoretical Division, T-3, Los Alamos National Laboratory, MA B216, Los Alamos, NM 87545, USA

Received 1 April 2003; received in revised form 18 June 2004
Available online 25 August 2004

Abstract

A new, two-dimensional (2D) homogenization theory is proposed. The theory utilizes a higher-order, elasticity-based cell model (ECM) analysis. The material microstructure is modeled as a 2D periodic array of unit cells where each unit cell is discretized into four subregions (or subcells). The analysis utilizes a (truncated) eigenfunction expansion of up to fifth order for the displacement field in each subcell. The governing equations for the theory are developed by satisfying the pointwise governing equations of geometrically linear continuum mechanics exactly up through an order consistent with the order of the subcell displacement field. The formulation is carried out independently of any specified constitutive models for the behavior of the individual phases (in the sense that the general governing equations hold for any constitutive model). The fifth order theory is subsequently specialized to a third order theory. Additionally, the higher order analyzes reduce to a theory equivalent to the original 2D method of cells (MOC) theory when all higher order terms are eliminated. The proposed 2D theory is the companion theory to an equivalent 3D theory [T.O. Williams, A three-dimensional, higher-order, elasticity-based micromechanics model, Int. J. Solids Struc., in press].

Comparison of the predicted bulk and local responses with published results indicates that the theory accurately predicts both types of responses. The high degree of agreement between the current theory results and published results is due to the correct incorporation of the coupling effects between the local fields.

The proposed theory represents the necessary theoretical foundations for the development of exact homogenization solutions of generalized, two-dimensional microstructures.

Keywords: Micromechanics; Elasticity-based cell model (ECM); Continuous fiber composites; Homogenization; Method of cells; Periodicity; Elasticity

* Tel.: +1 505 665 9190; fax: +1 505 665 5926.
E-mail address: oakhill@lanl.gov

0020-7683/$ - see front matter © 2004 Elsevier Ltd. All rights reserved.
doi:10.1016/j.ijsolstr.2004.06.057

1. Introduction

A current trend in the application of advanced materials is a greater emphasis on understanding the fundamental mechanisms governing the bulk response of the material. There are a multitude of reasons for this focus. For example, as structural applications become more demanding it is becoming increasingly important that the material microstructure be engineered in order to achieve specific response characteristics. Alternatively, in order to prevent catastrophic failure of a material during service, it is important that the mechanisms that drive the material failure be understood and, at least, predicted and, if possible, countered.

Inherent in the above requirement is the need to address the fact that all materials have microstructure. The heterogeneous nature of material microstructures give rise to complex interactions at this level. These interactions can drive critical local and bulk phenomena. In order to correctly predict these interactions it is necessary that material models provide accurate predictions for the local fields based on a knowledge of the microstructure and the properties of the individual components in the microstructure. Two dimensional microstructures composed of a doubly periodic array of inclusions represent one of the simplest possible material microstructures. Continuous fiber composites are one of the most common examples of such materials.

Two-dimensional micromechanical (or homogenization) theories represent a class of model especially well suited to the analysis of such materials. By their very nature these models provide predictions for the local behavior in different parts of a material's microstructure as well as providing estimates for the bulk response of a material system. These estimates are obtained by solving the appropriate governing equations of continuum mechanics subject to the constraints of the composite system's microstructural geometry and the response characteristics of the individual components composing a material system. Reviews of many of the existing 2D micromechanics models are given by Aboudi (1991), Christensen (1979), and Nemat-Nasser and Hori (1993).

The method of cells (MOC) (Aboudi, 1991) and its generalization, the generalized method of cells (GMC) (Paley and Aboudi, 1992) have proven to be particularly successful 2D micromechanical theories for modeling both the elastic and inelastic behavior of composite materials. Both theories discretize the material microstructure using rectangular subregions or subcells. The particular discretization used by the MOC theory is given in Fig. 1. Both of these theories are based on linear expansions for the displacement field within the subcells. The linear displacement expansion results in piecewise constant strain and stress fields within the subcells. Based on these expansions, the interfacial continuity conditions (for both displacements and tractions) are satisfied in an integral (or average) sense. The ability to formulate the general governing equations independently of any particular set of constitutive models enables the MOC/GMC theories to be utilized for inelastic analyzes with any desired set of constitutive models. Several studies have shown that the MOC/GMC theories provide accurate estimates for the bulk response of 2D composite systems (Lissenden and Herakovich, 1992; Noor and Shah, 1993). A review of the work (both elastic and inelastic) conducted using the MOC/GMC theories has been given by Aboudi (1996).

Despite the demonstrated ability of the MOC/GMC theories to model the bulk response of composites, a major issue in the use of the 2D MOC/GMC models is the lack of coupling between the local shearing and normal effects as well as between local shearing effects of different types. This lack has implications for the history-dependent analysis of composite materials, in particular, this lack can result in incorrect evolution of local history-dependent phenomena and, hence, of the bulk history-dependent behavior of the composite. The issue of the lack of coupling is addressed more fully by Williams and Aboudi (1999).

Several previous attempts have been made to address the lack of coupled local fields in the 2D MOC/GMC models. The first attempt (Williams and Aboudi, 1999) carried out a weak solution analysis based on a general expansion for the displacement field for a 2×2 unit cell (Fig. 1). Subsequently, the analysis was specialized to a third order form and reasonable comparison with existing results was obtained. A more recent attempt to address the issue has been pursued by Aboudi et al. (2001). In this model a partial, second

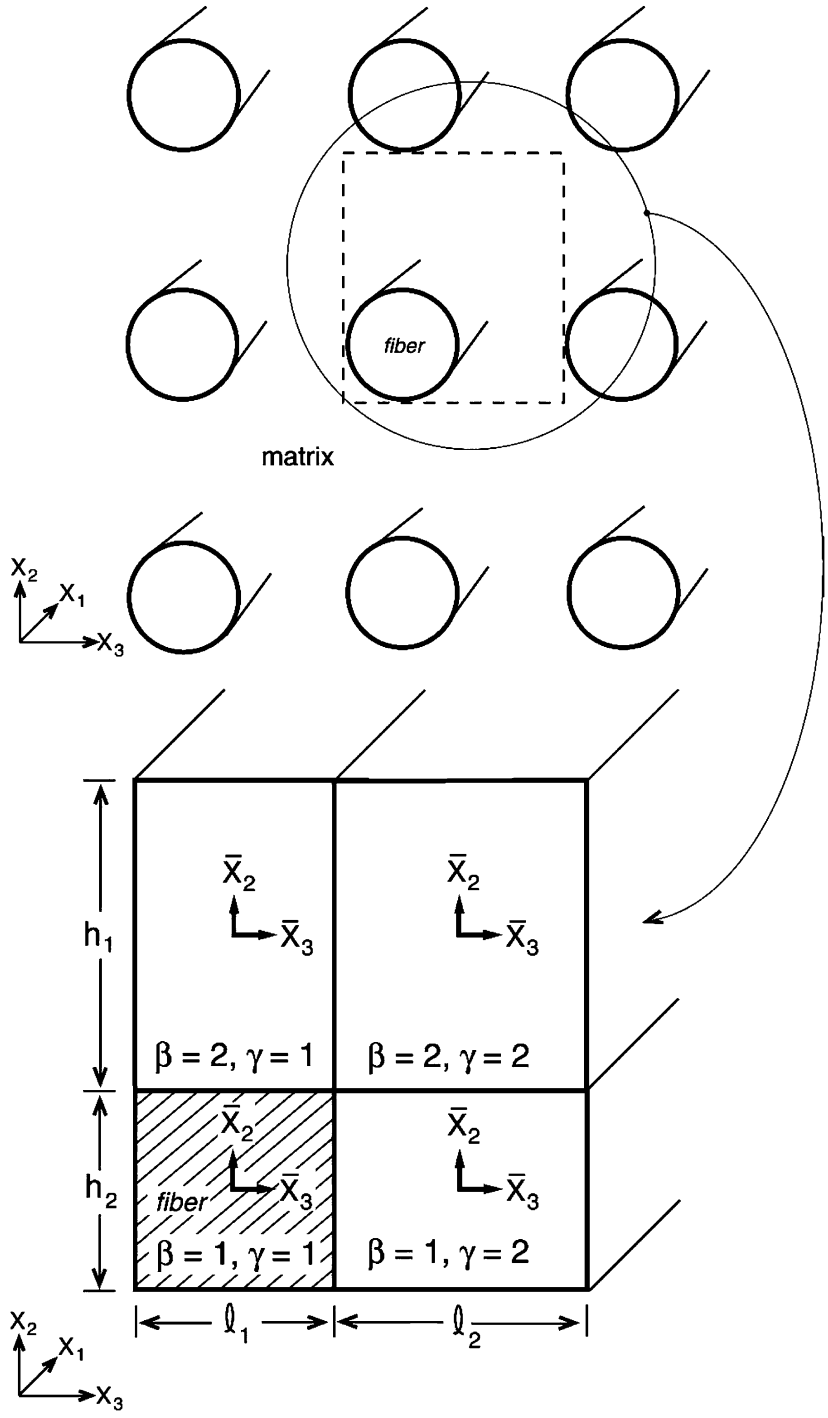

Fig. 1. The discretized unit cell for a continuous fiber composite used by both the original MOC model and the ECM.

order expansion for the displacement field within each subcell is used in conjunction with a weak formulation and the concepts of asymptotic homogenization (Bensoussan et al., 1978) to model the response of the composite.

There are a number of considerations associated with the above formulations. Common to both approaches is the use of weak formulations to obtain the governing equations. The formulations are "weak" in the sense that both formulations apply the method of moments to the pointwise equilibrium equations and subsequently use integration by parts in conjunction with the traction continuity conditions to arrive at the weak-form equilibrium equations. This type of approach has been shown to be consistent with a variational analysis, i.e. virtual work (Soldatos, 1995; Gilat, 1998) and thus the solution does not attempt to satisfy the pointwise governing equations. The theory developed by Williams and Aboudi (1999) introduced several overly stringent simplifying assumptions into the analysis through specializations of the interfacial traction continuity conditions. The more recent formulation by Aboudi et al. (2001) cannot be directly reduced to the original MOC/GMC formulations for several reasons. The first difference is that the theory cannot directly model the microstructure given in Fig. 1 since it is based on the concept of a generic cell (which is composed of four subcells; 2×2 subcells) and the analysis requires a minimum of two generic cells in a given direction (thus resulting in a minimum of four subcells in a given direction). The second difference is that the model is based on the use of asymptotic homogenization concepts which uses the concepts of asymptotic expansions. This introduces fundamental differences in the solution approach as compared to the MOC/GMC analyzes.

The purpose of the present paper is to present a new micromechanical model that is based on a higher-order, elasticity-based cell model (ECM) analysis. The proposed theory utilizes the same microstructural discretization as the original MOC model which assumes a doubly periodic array of unit cells where each unit cell is subdivided into four subregions or subcells (Fig. 1). The displacement field within each subcell is based on an eigenfunction expansion of up to fifth order. The strong form, i.e. the pointwise form, of the governing equations of geometrically linear continuum mechanics (equilibrium, traction continuity, and displacement continuity) are satisfied exactly up through an order consistent with the subcell displacement fields. The continuity constraints are satisfied both between subcells and between unit cells. The theory is formulated independently of the material constitutive relations for the individual phases in the sense that the governing equations do not depend on specific or special types of constitutive equations. The fifth order theory is subsequently specialized to a third order theory. Both of the higher order theories can be directly reduced to a variant of the original MOC analysis and have solution characteristics (for example providing all of the concentration tensors simultaneously) that are consistent with the original MOC formulation. The primary focus of the current paper is on the fundamental formulation of the 2D theory. For this purpose it is sufficient to consider only elastic behavior. The extension of the theory to inelastic analysis is only outlined in brief. This extension will be addressed more fully in future work.

Both the third and fifth order theories are validated by comparison with published results obtained from both finite element simulations and Green's function analyzes. It is shown that both ECM formulations can accurately predict the bulk elastic properties of continuous fiber composites and the local fields in the microstructure.

It is useful to put the proposed theory in perspective with respect to other types of micromechanical analyzes. While average field theories (such as those based on Eshelby, 1957, e.g. the Mori–Tanaka theory (Benveniste, 1987)) can adequately predict the effective elastic behavior of heterogeneous materials these types of theories are not capable of accurately predicting the effective inelastic behavior of such materials due to their inability to predict fluctuating fields about the phase average responses within the microstructure. In order to correctly predict these fluctuating responses, which drive the initiation and evolution of history-dependent behavior (see for example Williams and Pindera, 1997), it is necessary to employ homogenization theories capable of predicting spatially varying field effects within each phase. Some simplified theories (frequently referred to as cell models) attempt to obtain more accurate representations of the local

fields by selectively employing isostrain and/or isostress assumptions in localized subregions. These types of approaches do not, in general, correctly satisfy all of the governing equations of continuum mechanics or exhibit coupling of the local shear and normal fields (which is one of the major issues addressed within the current theory). In order to obtain accurate estimates of the local fluctuating fields, and, hence, of the global inelastic response, it is necessary to consider substantially more sophisticated theories. These approaches can be roughly separated into two different classes. The first class of approaches are analytical and are based on satisfying the governing equations of continuum mechanics in a strong sense, i.e. solving these equations in a pointwise fashion. Examples of such types of approaches are elasticity based solutions (see for example Williams and Pindera, 1995, 1997) or Green's function based analyzes (see Walker et al., 1993; Nemat-Nasser and Hori, 1993). The second class of approaches are numerical in nature. In general, this class of techniques satisfies the governing equations in a weak (variational) sense. Examples of these types of techniques are finite element based analyzes (both conventional and periodic). Both classes of techniques represent viable approaches to analyzing the homogenized response of heterogeneous materials with each class having different strengths and weaknesses. The proposed theory falls within the first class.

The proposed theory has a number of strengths and weaknesses when compared to other theories in the two different classes mentioned above. In general, analytical theories have a number of advantages over numerical approaches. These types of theories can be used to study local interaction effects in the microstructure that are not necessarily easily considered within the context of FE analyzes. Second, the first class of theories can provide analytical expressions for all of the mechanical and eigenstrain concentration tensors directly and simultaneously. Alternatively, the evaluation of the concentration tensors using numerical approaches requires a sequential application of the numerical analysis; one for each potential loading state, which in the case of history-dependent behavior can involve substantial computational cost. Third, analytical approaches can be used to study functional relations within the concentration tensors and, hence, the influence of different aspects the microstructure or the phase properties have on the local and bulk material response. Finally, due to their ability to generate the concentration tensors in analytical form and simultaneously, analytical models can be used to study functional forms for the bulk constitutive relations while this process is substantially more difficult within the context of FE based analyzes. Since the proposed approach falls within the first class of analyzes it has all of the above outlined advantages.

Numerical approaches have important strengths in their abilities to deal with complex microstructures subjected to complex loading states. Many analytical models do not have these capabilities and are specialized to the analysis of certain types of bulk loading or to specific microstructural geometries (see Williams and Pindera, 1995, 1997 for example). While the current variant of the proposed theory is limited to the analysis of rather specialized microstructures, the approach forms the cornerstone for the development of exact elasticity based analyzes for arbitrary microstructures based on infinite series solutions (developed in future work). The development of this cornerstone represents one of the most important contributions of the proposed theory. From a practical point of view the proposed solutions given in the following development represent the lowest order, truncated solutions in the infinite series solution that correctly couple the local fields. It is noted that when applicable exact solutions are obviously highly desirable.

The current theory has a number of other capabilities that should be recognized. The current model is sufficiently computationally efficient (in terms of the number of basic unknowns) that it can be implemented into structural analysis codes as a material constitutive model. The author's experience has shown the current approach to be more computationally efficient than some other elasticity based analyzes such as the concentric cylinders model for inelastic behavior (Williams and Pindera, 1995, 1997). The proposed theory's computationally efficiency can be significantly enhanced (by a reduction in the number of unknowns of almost 50%) by reformulating the governing equations using the local–global stiffness matrix (LGSM) approach (Williams and Pindera, 1995, 1997). The application of the LGSM reformulation to the proposed theory will be carried out in future work. Furthermore, an alternative to implementing the full form of the

proposed theory into structural analysis codes can be developed by utilizing the theory's ability to generate increasingly more accurate estimates for local piecewise uniform fields without the need to solve for the higher order terms in the theory (addressed in future work). Following this approach results in a substantial reduction in the number of unknowns with a corresponding increase in computational efficiency. The use of local piecewise uniform fields as the basis for estimates for bulk material behavior is a common practice in the implementation of homogenization concepts into structural analysis codes. Finally, the proposed theory can be employed in a sequential fashion by switching from lower order analyzes to higher order analyzes (and vice versa) on the fly. This last capability has obvious implications for both accuracy and computation efficiency as well as being the basis for considering convergence behavior as loading progresses for inelastic analyzes.

2. Theoretical framework for a fifth order theory

The following conventions are used throughout the formulation. Summation is implied on Latin alphabetic and Arabic numeric subscripts and superscripts. An overbar denotes a mean (volume averaged) field. For some generic field f this mean field is related to the pointwise field by

$$\bar{f} = \frac{1}{V}\int f \, \mathrm{d}V$$

where V is the volume of the unit cell. The associated (pointwise) fluctuating field is given by

$$f' = f - \bar{f}$$

By definition the fluctuating field has a zero mean ($\bar{f}' = 0$).

Various field expansions are utilized in the following formulation. The quantities on the left-hand side of these equations, $u_i^{(\beta,\gamma)}$ in Eq. (2.2), $\epsilon_{ij}^{(\beta,\gamma)}$ in Eq. (2.3), and $\sigma_{ij}^{(\beta,\gamma)}$ in Eq. (2.4), denote the pointwise value of the field within the (β,γ) subcell (Fig. 1). The different constants in these field expansions are denoted by the $V_{i(n,r)}^{(\beta,\gamma)}$ in Eq. (2.2), the $\mu_{ij(q,s)}^{(\beta,\gamma)}$ in Eq. (2.3), and $\sigma_{ij(q,s)}^{(\eta,\gamma)}$ in Eq. (2.4). The subscripts (n,r) or (q,s) denote the order of the constant, i.e. the associated order of the expansion functions. The superscripts (β,γ) denote the associated subcell (in the unit cell) in which the field expansion exists where β and γ range from 1 to 2 individually. When feasible the superscripts β and γ are dropped. In these circumstances it is to be understood that the associated discussion applies to all subcells. A local coordinate system $\overline{\boldsymbol{x}}$ is defined at the center of each subcell.

2.1. Subcell fields

Consider a doubly periodic array of inclusions embedded in a matrix (Fig. 1). The composite system is considered to be subjected to a displacement field of the form

$$U_i = \overline{\epsilon}_{ij} x_j \tag{2.1}$$

where the $\overline{\epsilon}_{ij}$ are the bulk (average) strains in the composite and the x_j are the macroscopic coordinates in the composite.

Given this type of material microstructure and global loading state it is sufficient to analyze only a *single* repeating unit cell (Fig. 1) due to the implied periodicity of the local fields. Following Aboudi (1991) this unit cell is subdivided into four subregions or subcells. Each subcell is considered to be occupied by a single

material. In general, at least one of the subcells will be occupied by the material which is considered to be the inclusion phase with the remaining subcells occupied by the matrix material. Note that if all of the subcells are occupied by the same material then the material is a homogeneous material and the proposed theory predicts that all fluctuating field effects are identically zero as required.

The assumed displacement field in a subcell is given by

$$u_i^{(\beta,\gamma)} = \bar{\epsilon}_{ij} x_j + P_{(n,r)} V_{i(n,r)}^{(\beta,\gamma)} \tag{2.2}$$

where

$$P_{(n,r)} = p_n(\bar{x}_2) p_r(\bar{x}_3)$$

and the $p_n(\bar{x}_2)$ are dimensional Legendre functions of order n in $\bar{x}_2$, the $p_r(\bar{x}_3)$ are dimensional Legendre functions of order r in $\bar{x}_3$, the $\bar{x}_i$ represent the local coordinates in the subcell, n and r range from 1 to 5 individually, and the cumulative order, denoted by $n + r$, must be an odd number (i.e. 1, 3, or 5). The particular forms for the dimensional Legendre polynomials are given in Appendix A. As mentioned above, summation is assumed on the subscripts n and r. The $V_{i(n,r)}^{(\beta,\gamma)}$ terms represent fluctuating displacement effects about the applied displacement field (Eq. (2.1)). These fluctuating displacement effects are induced by the presence of the material microstructure. The requirements that the local stress/strain fields be independent of the axial coordinate and that the fluctuating displacement field satisfy the continuity constraints results in the fact that the fluctuating displacement terms are independent of the axial coordinate x_1. There are 36 kinematic unknowns per subcell in a fifth order expansion giving a total of 144 unknowns in the unit cell. Eq. (2.2) is written out in expanded form in Appendix A.

The terms associated with even cumulative orders $(n + r)$ in the displacement expansion, Eq. (2.2), have been dropped since it can be shown that for the given microstructure, in conjunction with the field periodicity, these terms decouple from the odd cumulative order effects (both mean and fluctuating) and, hence, are identically zero. An example showing this decoupling process for the continuity equations is given in Appendix A. Inspection shows that the equilibrium equations (given in Section 2.2) are inherently decoupled. All of the forcing effects due to the applied bulk loading, Eq. (2.1), appear only in the governing equations associated with the odd cumulative order $(n + r)$ displacement field. The fact that all forcing effects associated with the even cumulative order displacement terms are identically zero results in only the trivial solution for these types of terms.

Note that any set of orthogonal (or even nonorthogonal) expansion functions could have been used in the formulation; Legendre polynomials simply represent a convenient choice. Use of different expansion functions would result only in changes in the coefficients in the basic governing equations but would not change the fundamental concepts behind the proposed analysis and hence the fundamental orders of the governing equations.

Substituting the subcell displacement field, Eq. (2.2), into the geometrically linear strain–displacement relations

$$\epsilon_{ij} = \frac{1}{2}(\partial_j u_i + \partial_i u_j)$$

gives a subcell strain field of the form

$$\epsilon_{ij}^{(\beta,\gamma)} = P_{(q,s)} \epsilon_{ij(q,s)}^{(\beta,\gamma)} = P_{(0,0)} \bar{\epsilon}_{ij} + P_{(q,s)} \mu_{ij(q,s)}^{(\beta,\gamma)} \tag{2.3}$$

where q and s range from 0 to 4 individually and the cumulative order, $q + s$, must be an even number (i.e. 0, 2, or 4). The fact that the cumulative order, $q + s$, for the strains must be an even number is consistent with the fact that only odd cumulative order $(n + r)$ terms exist in the displacement expansion, Eq. (2.2), which upon differentiation lead to strains of even cumulative order. The terms $\mu_{ij(q,s)}^{(\beta,\gamma)}$ represent

the fluctuating strain effects in the microstructure. These terms are defined in Appendix A. The expanded version of Eq. (2.3) is given in Appendix A.

The associated subcell stress field is given by

$$\sigma_{ij}^{(\beta,\gamma)} = P_{(q,s)}\sigma_{ij(q,s)}^{(\beta,\gamma)} \tag{2.4}$$

where $\sigma_{ij(q,s)}^{(\beta,\gamma)}$ are the stress terms in each subcell associated with the expansion functions $P_{(q,s)}$. The expanded version of Eq. (2.4) is given in Appendix A.

The following formulation is carried out independently of any particular set of constitutive relations for the behavior of the materials in the different subcells. Hence, the theory is applicable to any set of constitutive relations that relate the strain field, Eq. (2.3), to the stress field, Eq. (2.4). However, to determine the unknowns in the theory, the $V_{i(n,r)}^{(\beta,\gamma)}$, particular constitutive relations do have to be specified ultimately. Once a particular set of constitutive relations for the material in a subcell has been specified the subcell stress field can be directly written in terms of the kinematic unknowns, $V_{i(n,r)}^{(\beta,\gamma)}$, in the displacement field expansion (and appropriate history-dependent effects, for example, plastic strains). For example, in the case of linear elastic constituents the following constitutive relations can be obtained:

$$\sigma_{ij(q,s)}^{(\beta,\gamma)} = C_{ijkl}^{(\beta,\gamma)}\epsilon_{kl(q,s)}^{(\beta,\gamma)}$$

where the $C_{ijkl}^{(\beta,\gamma)}$ are the components of the stiffness tensor in a subcell. Using the expressions for the strain terms $\mu_{ij(q,s)}^{(\beta,\gamma)}$ (given in Appendix A) the stress terms $\sigma_{ij(q,s)}^{(\beta,\gamma)}$ can be directly expressed as functions of the fundamental unknowns, the $V_{i(n,r)}^{(\beta,\gamma)}$. The resulting relations can be subsequently substituted into the governing equations developed in the following formulation in order to express these equations solely in terms of the kinematic unknowns. If the more general form for the Hookean relations given by

$$\sigma_{ij} = C_{ijkl}\epsilon_{kl} + \lambda_{ij}$$

where the λ_{ij} represent eigenstress effects, is assumed then the particulars of the constitutive relations obviously change but the basic procedure for expressing the governing equations in terms of the kinematic unknowns remains unchanged. It is noted that a broad variety of constitutive relations, such as viscoelastic, plastic, and viscoplastic constitutive theories can be cast in the above form. For example, in a plasticity theory based on superposition of strain effects, the eigenstress is given by $\lambda_{ij} = -C_{ijkl}\epsilon_{kl}^{\mathrm{P}}$ where the $\epsilon_{kl}^{\mathrm{P}}$ are the plastic strains. The use of the above form for the constitutive relations does not preclude the necessity of incrementally evaluating the evolution of the internal state variables associated with the history-dependence.

2.2. Governing equations for the fifth order theory

The equilibrium equations for a subcell are obtained by substituting the subcell stress field, Eq. (2.4), into the pointwise (strong form) equilibrium equations,

$$\partial_2\sigma_{i2} + \partial_3\sigma_{i3} = 0$$

and collecting terms with the same spatial order and setting each group associated with the different spatial orders to zero. This process is equivalent to using the orthogonality properties of the expansion functions. The details of this process are given in Appendix A. The first cumulative order equilibrium equations in a subcell are given by

$$3\sigma_{i2(20)}^{(\beta,\gamma)} + \sigma_{i3(11)}^{(\beta,\gamma)} + 3\left(\frac{h_\beta}{2}\right)^2\sigma_{i2(40)}^{(\beta,\gamma)} + \left(\frac{l_\gamma}{2}\right)^2\sigma_{i3(13)}^{(\beta,\gamma)} = 0 \tag{2.5}$$

$$\sigma_{i2(11)}^{(\beta,\gamma)} + 3\sigma_{i3(02)}^{(\beta,\gamma)} + \left(\frac{h_\beta}{2}\right)^2 \sigma_{i2(31)}^{(\beta,\gamma)} + 3\left(\frac{l_\gamma}{2}\right)^2 \sigma_{i3(04)}^{(\beta,\gamma)} = 0 \tag{2.6}$$

where h_β and l_γ denote the lengths of the sides along the x_2 and x_3 directions of the (β,γ) subcell (see Fig. 1). The third cumulative order equilibrium equations within a subcell are given by

$$7\sigma_{i2(40)}^{(\beta,\gamma)} + \sigma_{i3(31)}^{(\beta,\gamma)} = 0 \tag{2.7}$$

$$5\sigma_{i2(31)}^{(\beta,\gamma)} + 3\sigma_{i3(22)}^{(\beta,\gamma)} = 0 \tag{2.8}$$

$$3\sigma_{i2(22)}^{(\beta,\gamma)} + 5\sigma_{i3(13)}^{(\beta,\gamma)} = 0 \tag{2.9}$$

$$\sigma_{i2(13)}^{(\beta,\gamma)} + 7\sigma_{i3(04)}^{(\beta,\gamma)} = 0 \tag{2.10}$$

There are six first order and 12 third order equilibrium equations per subcell giving a total of 72 equilibrium equations for the unit cell. That the above equilibrium equations are of odd cumulative order is due to the fact that they are based directly on the pointwise form of the equilibrium equations which require spatial differentiation of the stress field (which are of even cumulative order) leading to odd order equations only. These equilibrium equations are associated only with the odd cumulative order kinematic terms. If even cumulative order terms had been included in the analysis additional equilibrium equations of zeroth and second cumulative order would have been obtained. In this case it can be shown that the even (zeroth and second) cumulative order equilibrium equations completely decouple from the odd (first and third) cumulative order equilibrium equations. This last point is made to further illustrate the decoupling of the local fields of different orders (even or odd cumulative order).

Next the displacement continuity equations are developed. The displacement continuity equations in the theory are obtained by substituting Eq. (2.2) into the pointwise form of the displacement continuity constraints

$$u_i^+ = u_i^-$$

(where the superscripts $-/+$ are used to denote the different sides of an interface) and grouping the spatially varying effects of the same order and setting each group to zero. Again this is equivalent to using the orthogonality properties of the expansion functions. See Appendix A for example manipulations. The displacement continuity equations are imposed up through a cumulative order of two across the faces of the subcells and unit cells. For faces with the normal in the x_2-direction the appropriate displacement continuity equations are

$$\frac{h_1}{2} V_{i(10)}^{(1,\gamma)} + \left(\frac{h_1}{2}\right)^3 V_{i(30)}^{(1,\gamma)} + \left(\frac{h_1}{2}\right)^5 V_{i(50)}^{(1,\gamma)} = -\frac{h_2}{2} V_{i(10)}^{(2,\gamma)} - \left(\frac{h_2}{2}\right)^3 V_{i(30)}^{(2,\gamma)} - \left(\frac{h_2}{2}\right)^5 V_{i(50)}^{(2,\gamma)} \tag{2.11}$$

$$V_{i(01)}^{(1,\gamma)} + \left(\frac{h_1}{2}\right)^2 V_{i(21)}^{(1,\gamma)} + \left(\frac{h_1}{2}\right)^4 V_{i(41)}^{(1,\gamma)} = V_{i(01)}^{(2,\gamma)} + \left(\frac{h_2}{2}\right)^2 V_{i(21)}^{(2,\gamma)} + \left(\frac{h_2}{2}\right)^4 V_{i(41)}^{(2,\gamma)} \tag{2.12}$$

$$\frac{h_1}{2} V_{i(12)}^{(1,\gamma)} + \left(\frac{h_1}{2}\right)^3 V_{i(32)}^{(1,\gamma)} = -\frac{h_2}{2} V_{i(12)}^{(2,\gamma)} - \left(\frac{h_2}{2}\right)^3 V_{i(32)}^{(2,\gamma)} \tag{2.13}$$

For faces with the normal in the x_3-direction the appropriate displacement continuity equations are

$$\frac{l_1}{2} V_{i(01)}^{(\beta,1)} + \left(\frac{l_1}{2}\right)^3 V_{i(03)}^{(\beta,1)} + \left(\frac{l_1}{2}\right)^5 V_{i(05)}^{(\beta,1)} = -\frac{l_2}{2} V_{i(01)}^{(\beta,2)} - \left(\frac{l_2}{2}\right)^3 V_{i(03)}^{(\beta,2)} - \left(\frac{l_2}{2}\right)^5 V_{i(05)}^{(\beta,2)} \tag{2.14}$$

$$V^{(\beta,1)}_{i(10)} + \left(\frac{l_1}{2}\right)^2 V^{(\beta,1)}_{i(12)} + \left(\frac{l_1}{2}\right)^4 V^{(\beta,1)}_{i(14)} = V^{(\beta,2)}_{i(10)} + \left(\frac{l_2}{2}\right)^2 V^{(\beta,2)}_{i(12)} + \left(\frac{l_2}{2}\right)^4 V^{(\beta,2)}_{i(14)} \tag{2.15}$$

$$\frac{l_1}{2} V^{(\beta,1)}_{i(21)} + \left(\frac{l_1}{2}\right)^3 V^{(\beta,1)}_{i(23)} = -\frac{l_2}{2} V^{(\beta,2)}_{i(21)} - \left(\frac{l_2}{2}\right)^3 V^{(\beta,2)}_{i(23)} \tag{2.16}$$

There are 36 interfacial displacement continuity equations for the unit cell. The above forms for the displacement continuity equations have been obtained by directly using the displacement expansion, Eq. (2.2). Due to the nature of the chosen microstructural representation, Eqs. (2.11)–(2.16) satisfy the continuity constraints between subcells within a unit cell as well as between unit cells, i.e. these equations explicitly satisfy all of the periodicity constraints of the problem. Note that if the even cumulative order kinematic terms had been included in the analysis the resulting continuity equations between the subcells and unit cells could have been manipulated in such a way as to completely decouple the even and odd cumulative order effects (see Appendix A).

The development of the traction continuity constraints directly parallels that of the development of the displacement continuity conditions, Eqs. (2.11)–(2.16). In particular, the subcell stress field, Eq. (2.4), is substituted into the pointwise traction continuity relations

$$t_i^+ = -t_i^-$$

The effects with the same spatial dependencies are subsequently grouped and each spatial grouping is set to zero. Consistent with the displacement continuity conditions, the traction continuity conditions between subcells and unit cells are applied up through a cumulative order of two. For faces with the normal in the x_2-direction the appropriate traction continuity equations are

$$\sigma^{(1,\gamma)}_{i2(00)} + \left(\frac{h_1}{2}\right)^2 \sigma^{(1,\gamma)}_{i2(20)} + \left(\frac{h_1}{4}\right)^4 \sigma^{(1,\gamma)}_{i2(40)} = \sigma^{(2,\gamma)}_{i2(00)} + \left(\frac{h_2}{2}\right)^2 \sigma^{(2,\gamma)}_{i2(20)} + \left(\frac{h_2}{2}\right)^4 \sigma^{(2,\gamma)}_{i2(40)} \tag{2.17}$$

$$\frac{h_1}{2}\sigma^{(1,\gamma)}_{i2(11)} + \left(\frac{h_1}{2}\right)^3 \sigma^{(1,\gamma)}_{i2(31)} = -\frac{h_2}{2}\sigma^{(2,\gamma)}_{i2(11)} - \left(\frac{h_2}{2}\right)^3 \sigma^{(2,\gamma)}_{i2(31)} \tag{2.18}$$

$$\sigma^{(1,\gamma)}_{i2(02)} + \left(\frac{1}{2}\right)^2 \sigma^{(1,\gamma)}_{i2(22)} = \sigma^{(2,\gamma)}_{i2(02)} + \left(\frac{h_1}{2}\right)^2 \sigma^{(2,\gamma)}_{i2(22)} \tag{2.19}$$

For faces with the normal in the x_3-direction the appropriate traction continuity equations are

$$\sigma^{(\beta,1)}_{i3(00)} + \left(\frac{l_1}{2}\right)^2 \sigma^{(\beta,1)}_{i3(02)} + \left(\frac{l_1}{2}\right)^4 \sigma^{(\beta,1)}_{i3(04)} = \sigma^{(\beta,2)}_{i3(00)} + \left(\frac{l_2}{2}\right)^2 \sigma^{(\beta,2)}_{i3(02)} + \left(\frac{l_2}{2}\right)^4 \sigma^{(\beta,2)}_{i3(04)} \tag{2.20}$$

$$\frac{l_1}{2}\sigma^{(\beta,1)}_{i3(11)} + \left(\frac{l_1}{2}\right)^3 \sigma^{(\beta,1)}_{i3(13)} = -\frac{l_2}{2}\sigma^{(\beta,2)}_{i3(11)} - \left(\frac{l_2}{2}\right)^3 \sigma^{(\beta,2)}_{i3(13)} \tag{2.21}$$

$$\sigma^{(\beta,1)}_{i3(20)} + \left(\frac{l_1}{2}\right)^2 \sigma^{(\beta,1)}_{i3(22)} = \sigma^{(\beta,2)}_{i3(20)} + \left(\frac{l_2}{2}\right)^2 \sigma^{(\beta,2)}_{i3(22)} \tag{2.22}$$

There are 36 interfacial traction continuity equations for the unit cell. As was the case for the displacement continuity equations, the above form of the traction continuity conditions satisfy continuity both between subcells within a unit cell and continuity between unit cells. Thus, these equations explicitly satisfy the all traction constraints on the local fields. Also, in parallel with the displacement continuity conditions, if even cumulative order effects ($q + s$) had been included the traction continuity equations could have been

manipulated so as to separate the even and odd cumulative order effects (see Appendix A). The bulk (average) strains which represent the forcing effects in the theory enter into the problem through the zeroth order stresses only. Since the forcing terms associated with the odd cumulative order stress effects (which are functions of the even cumulative order displacement effects) are identically zero the even cumulative order displacement effects must be zero.

2.3. Implementation of the governing equations

The governing equations, Eqs. (2.5)–(2.22), represent 144 governing equations for the 144 kinematic unknowns, $V_{i(n,r)}^{(\beta,\gamma)}$. These governing equations are algebraic in nature and thus can be directly assembled into matrix form by simply considering each governing equation given above to represent one line in the matrix equation. In particular, Eqs. (2.11)–(2.16) (the displacement continuity equations) are used as presented. The stresses can be expressed in terms of the kinematic unknowns by using the process discussed in Section 2.1. Subsequent substitution of these results into Eqs. (2.5)–(2.10) and (2.17)–(2.22) results in expressions of the equilibrium equations and the traction continuity equations given in terms of the fundamental unknown kinematic terms. If elastic Hookean behavior is assumed for the constituents the governing equations can be written in the following matrix form:

$$\underline{\underline{K}}\,\underline{V} = \underline{\underline{F}}\,\underline{\bar{\epsilon}} \tag{2.23}$$

where $\underline{\underline{K}}$ is a coefficient matrix that is a known function of the material and geometric properties of the subcells, the vector of unknowns for the unit cell is given by $\underline{V}$, the matrix $\underline{\underline{F}}$ is associated with the forcing terms and is a known function of the material and geometric properties of the subcells, and the vector $\underline{\bar{\epsilon}}$ represents the applied bulk loading. If the constituents are assumed to exhibit history-dependent responses then additional terms would appear in the above matrix equation in the form of an additional forcing vector on the right-hand side. This extension to history-dependent effects will be addressed in future work.

2.4. Specialization of governing equations for orthotropic phases

Careful consideration of the governing equations for Hookean materials with at least orthotropic symmetry indicates that the kinematic unknowns and the governing equations can be separated into four independent groupings. This separation of the fundamental unknowns results in significantly smaller systems of equations that need to be solved and, thus, has implications for the computational efficiency of the theory. It is noted that most typical composites used in structural applications exist within this class of materials.

The first independent grouping (henceforth referred to as group 1) of the kinematic unknowns is given by; $V_{1(10)}$, $V_{1(12)}$, $V_{1(14)}$, $V_{1(30)}$, $V_{1(32)}$, $V_{1(50)}$. There are a total of 24 unknowns for the unit cell in this group. The associated stresses are given by; $\sigma_{12(00)}$, $\sigma_{12(02)}$, $\sigma_{12(04)}$, $\sigma_{12(20)}$, $\sigma_{12(22)}$, $\sigma_{12(40)}$, $\sigma_{13(11)}$, $\sigma_{13(13)}$, and $\sigma_{13(31)}$. The governing equations for group 1 are given by Eqs. (2.5), (2.7), (2.9), (2.11), (2.13), (2.15), (2.17), (2.19), and (2.21) all with the free index $i = 1$.These equations represent a consistent system of 24 equations for the 24 unknowns. Examination shows that the behavior in group 1 is driven by the applied bulk strain $\bar{\epsilon}_{12}$, i.e. one of the axial shear components. Both types of *local* axial shear (12 as well as 13) effects exist within the group and their evolution is coupled. The 13 shear effects only exist as higher order effects with a zero average while the 12 shear effects affect both the average response associated with group 1 as well as higher order effects (as is consistent with expectations). The governing equations for the group can be expressed in the following form:

$$\underline{\underline{k}}^{(1)}\underline{V}^{(1)} = \underline{f}^{(1)}\bar{\epsilon}_{12} \tag{2.24}$$

where the superscript (1) denotes the group number, $\underline{\underline{k}}^{(1)}$ is a coefficient matrix composed of the known geometric and material properties of the subcells and the unit cells, $\underline{V}^{(1)}$ is the vector of unknowns for the group, and $\underline{f}^{(1)}$ is another vector composed of known quantities existing within the subcells and the unit cell.

The second independent grouping (referred to as group 2) is mathematically equivalent to group 1. The kinematic unknowns in this group are given by; $V_{1(01)}$, $V_{1(03)}$, $V_{1(05)}$, $V_{1(21)}$, $V_{1(23)}$, and $V_{1(41)}$. As in group 1 there are 24 unknowns for the unit cell for this group. The associated stresses are given by; $\sigma_{13(00)}$, $\sigma_{13(20)}$, $\sigma_{13(40)}$, $\sigma_{13(02)}$, $\sigma_{13(22)}$, $\sigma_{13(04)}$, $\sigma_{13(11)}$, $\sigma_{12(13)}$, and $\sigma_{12(31)}$. The governing equations for group 2 are given by Eqs. (2.6), (2.8), (2.10), (2.12), (2.14), (2.16), (2.18), (2.20) and (2.22) all with the free index $i = 1$. These equations provide 24 governing equations for the 24 unknowns within the group. The responses within group 2 are driven by the other applied bulk axial shear strain, $\overline{\epsilon}_{13}$. As was the case in group 1, both *local* 12 and 13 shearing responses exist within group 2. However, in this case, the roles of the effects are reversed with 12 effects only existing as higher order effects and the 13 effects impacting both the average and higher order responses. The governing equations for the group can be written in the same form as was done for group 1, i.e.

$$\underline{\underline{k}}^{(2)}\underline{V}^{(2)} = \underline{f}^{(2)}\overline{\epsilon}_{13} \tag{2.25}$$

where the superscript 2 denotes the group number. The interpretations of the terms in the above equation exactly parallel those of group 1.

Both groups 1 and 2 are decoupled from any type of transverse shearing or normal responses (macroscopic or microscopic) as is consistent with expectations for a continuous fiber composite.

The third group is associated with the bulk transverse shearing response, $\overline{\epsilon}_{23}$. The microstructural kinematic terms in this group are given by; $V_{2(01)}$, $V_{2(03)}$, $V_{2(05)}$, $V_{2(21)}$, $V_{2(23)}$, $V_{2(41)}$, $V_{3(10)}$, $V_{3(12)}$, $V_{3(14)}$, $V_{3(30)}$, $V_{3(32)}$, and $V_{3(50)}$. There are a total of 48 unknowns in group 3. The corresponding stress terms are $\sigma_{23(00)}$, $\sigma_{23(02)}$, $\sigma_{23(05)}$, $\sigma_{23(20)}$, $\sigma_{23(22)}$, $\sigma_{23(40)}$, $\sigma_{nn(11)}$, $\sigma_{nn(13)}$, and $\sigma_{nn(31)}$ where the subscripts "*nn*" are used to denote the normal stresses (with no summation on *n*). The governing equations for group 3 are Eqs. $(2.5)_{i=3}$, $(2.6)_{i=2}$, $(2.7)_{i=3}$, $(2.8)_{i=2}$, $(2.9)_{i=3}$, $(2.10)_{i=2}$, $(2.11)_{i=3}$, $(2.12)_{i=2}$, $(2.13)_{i=3}$, $(2.14)_{i=2}$, $(2.15)_{i=3}$, $(2.16)_{i=2}$, $(2.17)_{i=3}$, $(2.18)_{i=2}$, $(2.19)_{i=3}$,$(2.20)_{i=2}$, $(2.21)_{i=3}$, and $(2.22)_{i=2}$ where the subscript on the equation number indicates the associated value of the free index *i*. There are 48 governing equations for the 48 total unknowns within group 3. The local responses within group 3 consist of both transverse shearing effects and normal effects. The transverse shearing responses represent both the average behavior associated with the group as well as higher order responses while the normal effects only exist as higher order phenomena. Again, the governing equations can be expressed in the form already seen for groups 1 and 2

$$\underline{\underline{k}}^{(3)}\underline{V}^{(3)} = \underline{f}^{(3)}\overline{\epsilon}_{23} \tag{2.26}$$

with the same interpretations for the individual terms in the matrix equation.

The last group, group 4, is driven by the bulk normal applied strains $\overline{\epsilon}_{11}$, $\overline{\epsilon}_{22}$, and $\overline{\epsilon}_{33}$. The kinematic unknowns for this group consist of the following terms; $V_{2(10)}$, $V_{2(12)}$, $V_{2(14)}$, $V_{2(30)}$, $V_{2(32)}$, $V_{2(50)}$, $V_{3(01)}$, $V_{3(03)}$, $V_{3(05)}$, $V_{3(21)}$, $V_{3(23)}$, and $V_{3(41)}$. There are 48 unknowns for the unit cell in group 4. The kinematic terms within this group give rise to the following stresses; $\sigma_{nn(00)}$, $\sigma_{nn(02)}$, $\sigma_{nn(04)}$, $\sigma_{nn(20)}$, $\sigma_{nn(22)}$, $\sigma_{nn(40)}$, $\sigma_{23(11)}$, $\sigma_{23(13)}$, and $\sigma_{23(31)}$. There are 48 governing equations in group 4 given by Eq. $(2.5)_{i=1}$, $(2.6)_{i=3}$, $(2.7)_{i=2}$, $(2.8)_{i=3}$, $(2.9)_{i=2}$, $(2.10)_{i=3}$, $(2.11)_{i=2}$, $(2.12)_{i=3}$, $(2.13)_{i=2}$, $(2.14)_{i=3}$, $(2.15)_{i=2}$, $(2.16)_{i=3}$, $(2.17)_{i=2}$, $(2.18)_{i=3}$, $(2.19)_{i=2}$, $(2.20)_{i=3}$, $(2.21)_{i=2}$, and $(2.22)_{i=3}$. As was the case in group 3, both local transverse shearing and normal responses are present within group 4. However, in the current case, the roles of these effects can be considered to be reversed as compared to group 3. In particular, the local normal effects affects both the average behavior as well as higher order responses while the transverse shearing terms only exist within

the context of higher order effects. The governing equations for this group can be expressed in a similar form as observed for the other groups.

$$\underline{\underline{k}}^{(4)}\underline{V}^{(4)} = \underline{\underline{f}}^{(4)}\overline{\underline{\epsilon}}^{n} \tag{2.27}$$

where the interpretation of the individual terms in the equation directly parallel those used in the other groups with the exception that the vector $\overline{\underline{\epsilon}}_n$ consists of the three bulk normal strains $\overline{\epsilon}_{11}$, $\overline{\epsilon}_{22}$, and $\overline{\epsilon}_{33}$, and $\underline{\underline{f}}^{(4)}$ is a matrix composed of known quantities.

The concentration factors effects for the kinematic unknowns can be directly determined from Eqs. (2.23)–(2.26). In particular, have

$$\underline{V}^{(1)} = \underline{\underline{k}}^{(1)^{-1}}\underline{f}^{(1)}\overline{\epsilon}_{12} = \underline{a}^{(1)}\overline{\epsilon}_{12} \tag{2.28}$$

$$\underline{V}^{(2)} = \underline{\underline{k}}^{(2)^{-1}}\underline{f}^{(2)}\overline{\epsilon}_{13} = \underline{a}^{(2)}\overline{\epsilon}_{13} \tag{2.29}$$

$$\underline{V}^{(3)} = \underline{\underline{k}}^{(3)^{-1}}\underline{f}^{(3)}\overline{\epsilon}_{23} = \underline{a}^{((3))}\overline{\epsilon}_{23} \tag{2.30}$$

$$\underline{V}^{(4)} = \underline{\underline{k}}^{(4)^{-1}}\underline{\underline{f}}^{(4)}\overline{\underline{\epsilon}}_{n} = \underline{\underline{a}}^{(4)}\overline{\underline{\epsilon}}_{n} \tag{2.31}$$

where the vectors $\underline{a}^{(i)}$ for $i = 1,2,3$ and the matrix $\underline{\underline{a}}^{(4)}$ represent the concentration tensor effects. Note that the above results are closed form, analytic expressions for the concentration factors.

Based on the above results the fluctuating strain terms $\mu_{ij(q,s)}^{(\beta,\gamma)}$ can be expressed in the following form:

$$\mu_{ij(q,s)}^{(\beta,\gamma)} = A_{ijkl(q,s)}^{(\beta,\gamma)}\overline{\epsilon}_{kl} \tag{2.32}$$

where the $A_{ijkl(q,s)}^{(\beta,\gamma)}$ are the concentration tensors. These tensors are direct functions of the previously determined vectors $\underline{a}^{(i)}$ for $i = 1,2,3$ and the matrix $\underline{\underline{a}}^{(4)}$.

2.5. Effective constitutive properties of the composite

The effective properties of the composite system can now be determined using the previous results. In the following discussion it is assumed that the constituents are Hookean materials such that the following constitutive relations hold in each phase:

$$\sigma_{ij} = C_{ijkl}\epsilon_{kl} \tag{2.33}$$

where C_{ijkl} are the components of the stiffness tensor. In this situation the effective stiffnesses C_{ijkl}^{eff} are defined by

$$\overline{\sigma}_{ij} = C_{ijkl}^{\text{eff}}\overline{\epsilon}_{kl} \tag{2.34}$$

Separating all of the field quantities in Eq. (2.33) into mean and fluctuating parts and taking the mean of the result gives the following expression for the average constitutive relations:

$$\overline{\sigma}_{ij} = \overline{C}_{ijkl}\overline{\epsilon}_{kl} + \overline{C'_{ijkl}\mu_{kl}}$$

where the C'_{ijkl} are the components of the fluctuating stiffness tensor in the different subcells. Note that $\overline{C}_{ijkl}$ corresponds to the Voight (simple volume averaged) estimate for the effective stiffness tensor (see the definitions in Section 2). Substituting Eq. (2.32) into this expression gives

$$\overline{\sigma}_{ij} = \left(\overline{C}_{ijkl} + \overline{C'_{ijmn}A_{mnkl}}\right)\overline{\epsilon}_{kl}$$

where the A_{mnkl} are the concentration tensor components in the different subcells (see Eq. (2.32)). Comparison of this result with Eq. (2.34) shows that the effective stiffness tensor is given by

$$C^{\text{eff}}_{ijkl} = \overline{C}_{ijkl} + \overline{C'_{ijmn} A_{mnkl}} \tag{2.35}$$

In the case where the constitutive properties within the phases are spatially constant, i.e. do not vary as a function of position within the subcell, the above result simplifies to the following form:

$$C^{\text{eff}}_{ijkl} = \overline{C}_{ijkl} + \overline{C'_{ijmn} A_{mnkl(00)}} \tag{2.36}$$

Alternatively, Eq. (2.36) can be expressed in the form

$$C^{\text{eff}}_{ijkl} = \overline{C}_{ijkl} + \sum_{\beta,\gamma} c_{(\beta,\gamma)} C'^{(\beta,\gamma)}_{ijmn} A^{(\beta,\gamma)}_{mnkl(00)} \tag{2.37}$$

where the $c_{(\beta,\gamma)}$ are the subcell volume fractions, i.e. the relative volume of each subcell with respect to the total volume of the unit cell. Using standard relations the effective material properties can be obtained from Eqs. (2.35)–(2.37). Note that since the concentration factors are obtained from closed form, analytic expressions the effective properties for the composite are also given by closed form, analytic results.

3. Third order theory

This section deals with the appropriate reduction of the fifth order theory to a third order theory. Obviously the first step in this process is the elimination of all of the fifth cumulative order $(n + r)$ kinematic terms in the displacement expansion and all of the (associated) fourth cumulative order $(q + s)$ terms in the strain and stress field expansions. The resulting subcell displacement, strain, and stress fields after these reductions still retain the functional forms given in Eqs. (2.2)–(2.4), respectively. These reductions result in a total of 72 kinematic unknowns for the third order theory.

It can be seen that as a consequence of the elimination of the above higher order terms all of the third order equilibrium equations identically vanish. Thus, the only equilibrium equations remaining are the first order equilibrium equations, Eqs. (2.5) and (2.6). However, since the fourth order stress effects no longer exist these equations simplify to the following forms:

$$3\sigma^{(\beta,\gamma)}_{i2(20)} + \sigma^{(\beta,\gamma)}_{i3(11)} = 0 \tag{3.1}$$

$$\sigma^{(\beta,\gamma)}_{i2(11)} + 3\sigma^{(\beta,\gamma)}_{i3(02)} = 0 \tag{3.2}$$

There are a total of 24 governing equilibrium equations for the unit cell.

In the third order theory the displacement and traction continuity equations are imposed up through a cumulative order of one across the faces of the subcells and the unit cells. As was the case for the equilibrium equations the continuity constraints also simplify. In particular, the displacement continuity equations become

$$\frac{h_1}{2} V^{(1,\gamma)}_{i(10)} + \left(\frac{h_1}{2}\right)^3 V^{(1,\gamma)}_{i(30)} = -\frac{h_2}{2} V^{(2,\gamma)}_{i(10)} - \left(\frac{h_2}{2}\right)^3 V^{(2,\gamma)}_{i(30)} \tag{3.3}$$

$$V^{(1,\gamma)}_{i(01)} + \left(\frac{h_1}{2}\right)^2 V^{(1,\gamma)}_{i(21)} = V^{(2,\gamma)}_{i(01)} + \left(\frac{h_2}{2}\right)^2 V^{(2,\gamma)}_{i(21)} \tag{3.4}$$

$$\frac{l_1}{2}V^{(\beta,1)}_{i(01)} + \left(\frac{l_1}{2}\right)^3 V^{(\beta,1)}_{i(03)} = -\frac{l_2}{2}V^{(\beta,2)}_{i(01)} - \left(\frac{l_2}{2}\right)^3 V^{(\beta,2)}_{i(03)} \tag{3.5}$$

$$V^{(\beta,1)}_{i(10)} + \left(\frac{l_1}{2}\right)^2 V^{(\beta,1)}_{i(12)} = V^{(\beta,2)}_{i(10)} + \left(\frac{l_2}{2}\right)^2 V^{(\beta,2)}_{i(12)} \tag{3.6}$$

while the traction continuity equations are

$$\sigma^{(1,\gamma)}_{i2(00)} + \left(\frac{h_1}{2}\right)^2 \sigma^{(1,\gamma)}_{i2(20)} = \sigma^{(2,\gamma)}_{i2(00)} + \left(\frac{h_2}{2}\right)^2 \sigma^{(2,\gamma)}_{i2(20)} \tag{3.7}$$

$$\frac{h_1}{2}\sigma^{(1,\gamma)}_{i2(11)} = -\frac{h_2}{2}\sigma^{(2,\gamma)}_{i2(11)} \tag{3.8}$$

$$\sigma^{(\beta,1)}_{i3(00)} + \left(\frac{l_1}{2}\right)^2 \sigma^{(\beta,1)}_{i3(02)} = \sigma^{(\beta,2)}_{i3(00)} + \left(\frac{l_2}{2}\right)^2 \sigma^{(\beta,2)}_{i3(02)} \tag{3.9}$$

$$\frac{l_1}{2}\sigma^{(\beta,1)}_{i3(11)} = -\frac{l_2}{2}\sigma^{(\beta,2)}_{i3(11)} \tag{3.10}$$

There are 24 governing equations obtained from each of the displacement and traction continuity conditions, Eqs. (3.3)–(3.10).

Consideration of the above traction continuity equations shows that Eq. (3.8) for $i = 3$ and Eq. (3.10) for $i = 2$ only represent three independent governing equation. In order to obtain a deterministic system of governing equations for the third order theory it is necessary to impose the following spin constraint:

$$\sum_{\beta,\gamma} h^3_\beta l^3_\gamma \left(V^{(\beta,\gamma)}_{2(12)} - V^{(\beta,\gamma)}_{3(21)}\right) = 0 \tag{3.11}$$

instead of one of these traction continuity conditions. The above spin constraint equation is based on the fact that a homogeneous material subjected to the deformation field given by Eq. (2.1) has zero spin. It is noted that this type of constraint on the local average spins can be employed in the original MOC model to determine the nine fundamental displacement field unknowns instead of the six secondary unknown strains in a subcell.

The governing equations for the third order theory, Eqs. (3.1)–(3.11) provide a system of 72 equations for the 72 kinematic unknowns.

The groupings observed in the fifth order theory are also present in the third order theory when it is assumed that the constituent materials exhibit Hookean behavior with at least orthotropic symmetry. The remaining discussion in this section utilizes this fact.

For group 1 the kinematic terms that must be eliminated are; $V_{1(14)}$, $V_{1(32)}$, and $V_{1(50)}$, while the remaining kinematic terms are $V_{1(10)}$, $V_{1(12)}$, and $V_{1(30)}$. The associated governing equations are Eqs. (3.1), (3.3), (3.6), (3.7), and (3.10) all with $i = 1$.

The only remaining kinematic terms in group 2 are $V_{1(01)}$, $V_{1(03)}$, and $V_{1(21)}$. The appropriate governing equations are given by Eqs. (3.2), (3.4), (3.6), (3.8), and (3.9) all with $i = 1$.

There are 12 governing equations for the 12 kinematic unknowns in both groups 1 and 2.

The group 3 kinematic unknowns in the third order analysis are $V_{2(01)}$, $V_{2(03)}$, $V_{2(21)}$, $V_{3(10)}$, $V_{3(12)}$, and $V_{3(30)}$ which represent 24 unknowns. The corresponding governing equations are Eq. (3.1) with $i = 3$, Eqs. $(3.2)_{i=2}$, $(3.3)_{i=3}$, $(3.4)_{i=2}$, $(3.5)_{i=2}$, $(3.6)_{i=3}$, $(3.7)_{i=3}$, $(3.8)_{i=2}$, $(3.9)_{i=2}$, and $(3.10)_{i=3}$ which provide the necessary 24 governing equations.

Finally, for group 4 the kinematic terms $V_{2(10)}$, $V_{2(12)}$, $V_{2(30)}$, $V_{3(01)}$, $V_{3(03)}$, and $V_{3(21)}$ must be retained. Thus, there are 24 unknowns in group 4. The final set of 24 governing equations for this group are Eqs. $(3.1)_{i=2}$, $(3.2)_{i=3}$, $(3.3)_{i=2}$, $(3.4)_{i=3}$, $(3.5)_{i=3}$, $(3.6)_{i=2}$, $(3.7)_{i=2}$, $(3.8)_{i=3}$, $(3.9)_{i=3}$, and $(3.10)_{i=2}$.

The governing equations for groups 1–4 in the third order analysis directly parallel Eqs. (2.24)–(2.27) and as a consequence the concentration tensor effects can be obtained from equations similar to Eqs. (2.28)–(2.31). The strain field in the subcells can be expressed as in Eq. (2.32) where the maximum cumulative order is two. The expressions for the effective properties given previously, Eqs. (2.35)–(2.37), can be directly utilized in the third order analysis.

4. Specialization of the higher order theories to the MOC theory

The original MOC (Aboudi, 1991) model is based on a first order expansion for the displacement field within a subcell. To specialize the previous formulations to a variant of the MOC theory all third and fifth (cumulative) order kinematic terms are eliminated. The remaining kinematic terms are given by $V_{i(100)}$, $V_{i(010)}$, and $V_{i(001)}$ while the remaining stresses and fluctuating strains are simply given by $\sigma_{ij(00)}$ and $\mu_{ij(00)}$, respectively. The governing equations subsequently reduce to the average continuity equations only (without any higher order effects). As expected the groupings that exist in the higher order analyzes also exist in the first order analysis. Since a theory corresponding to the original MOC model can be obtained by specializing the current formulation, the MOC theory can be interpreted as a lowest order elasticity solution rather than a theory based on a weak formulation (which is how the original theory is presented).

5. Validation results

This section is intended to provide validation of the proposed modeling approach and is composed of two parts. The first part of the validation process is carried out by comparing the current model predictions for the effective moduli with various results from the open literature generated using finite element (FE) analyzes. The second part considers the accuracy of the predictions for the local fields by comparing the model's predictions with those obtained from a Green's function analysis (Walker et al., 1993). The method of cells predictions are also presented for comparison. In the following discussions the current theory with be referred to as the ECM.

The exact elasticity solution for a bilaminated material has been given by Aboudi (1991). The proposed elasticity based analysis has been numerically shown to correctly collapse to this solution (not shown). This result is a necessary condition in the validation of the proposed theory.

The effective elastic moduli predictions obtained from the current third ECM order analysis are compared to the FE based predictions for periodic hexagonal and square arrays generated by Sun and Vaidya (1996). The results of Sun and Vaidya where shown to be accurate through comparison with both experimental data and the predictions of various other models. It is noted that the work of Sun and Vaidya developed an FE tool that carried out the analysis based on periodic fields and boundary conditions. In the following discussion, particular attention should be paid to the comparison with the square array based FE predictions. The constituent properties are given in Table 1. It is noted that for the following examples that consider the bulk effective properties the ECM results are independent of the loading state. This is unlike FE based analyzes that require the implementation of six independent loading states in order to determine the effective properties. The first set of results to be considered are for a B/Al composite with a fiber volume fraction of 0.47 (Table 2). This material system is representative of typical large diameter, continuous fiber metal matrix composites. As expected the axial Young's modulus is accurately predicted by both the ECM theory as well as the MOC theory. The ECM model gives slightly better predictions for the

Table 1
Properties for boron, aluminum, AS4 graphite, and 3501-6 epoxy constituents (Sun and Vaidya, 1996)

Material	E_l (GPa)	E_t (GPa)	ν_{tt}	ν_{lt}	G_{tt} (GPa)	G_{lt} (GPa)
Boron	379.3	379.3	0.10	0.10	172.41	172.41
Aluminum	68.30	68.30	0.30	0.30	26.27	26.27
AS4 graphite	235.0	14.0	0.25	0.20	5.6	28.0
3501-6 epoxy	4.8	4.8	0.34	0.34	1.8	1.8

Table 2
Predicted effective properties for B/Al continuous fiber composite at a volume fraction of 0.47 (Sun and Vaidya, 1996)

Model	E_l (GPa)	E_t (GPa)	ν_{tt}	ν_{lt}	G_{tt} (GPa)	G_{lt} (GPa)
FE (square array)	215	144	0.29	0.19	45.9	57.2
FE (hexagonal array)	215	136.5	0.34	0.19	52.5	54.0
MOC	215	142.6	0.25	0.20	43.7	51.3
Third order ECM	215	143.4	0.26	0.19	45.1	54.3

effective transverse Young's moduli and Poisson's ratios than does the MOC model although both models under predict the effective transverse Poisson's ratio. Consideration of the shear moduli predictions indicates that the ECM model provides better predictions for these properties than does the MOC theory. The predictions for the transverse shear modulus obtained from the ECM are more accurate than the predictions for the axial shear moduli. The second composite system to be considered is a Gr/Ep system with a fiber volume fraction of 0.60 (Table 3). This Gr/Ep system is typical of the types of unidirectional composites being utilized in the majority of structural applications. Again, both the ECM and MOC theories accurately predict the axial Young's modulus. Both models also provide highly accurate predictions for the transverse Young's moduli and the Poisson's ratios. The ECM model can be seen to provide more accurate predictions for the axial effective shear modulus than obtained from the original MOC model.

Next, predictions for the effective elastic moduli of a Gr/Ep (Modmor II graphite/LY558 Epoxy), again typical of unidirectional composite materials used in applications, as a function of volume obtained from the current third order theory are compared to the corresponding finite element results generated by both Bennett and Haberman (1996) and Noor and Shah (1993). The work by Bennett and Haberman developed a micromechancial scheme that accounted for the effect of periodicity conditions on the local fields within the context of a finite element implementation. Their results were generated for a square fiber array. The analysis by Noor and Shah used standard finite element approaches to model the response of both square and hexagonal array microstructures. Noor and Shah carried out their analyzes using converged meshes. Their results compared well with a number of different micromechanics models. In the following discussion the results of Bennett and Haberman will be referred to as B–H while the Noor and Shah work will be referenced by N–S. The material properties for the constituents are given in Table 4. Note that the high

Table 3
Predicted effective properties for Gr/Ep continuous fiber composite at a volume fraction of 0.60 (Sun and Vaidya, 1996)

Model	E_l (GPa)	E_t (GPa)	ν_{tt}	ν_{lt}	G_{tt} (GPa)	G_{lt} (GPa)
FE (square array)	143	9.6	0.35	0.25	3.10	6.00
FE (hexagonal array)	143	9.2	0.38	0.25	3.35	5.88
MOC	143	9.6	0.35	0.25	3.08	5.47
Third order ECM	143	9.6	0.35	0.25	3.07	5.85

Table 4
Properties for Modmor II graphite and LY558 epoxy (Noor and Shah, 1993)

Material	E_l (GPa)	E_t (GPa)	ν_{tt}	ν_{lt}	G_{tt} (GPa)	G_{lt} (GPa)
Modmor II graphite	232.0	15.0	0.49	0.279	5.03	24.0
LY588 epoxy	5.35	5.35	0.354	0.354	1.976	1.8

contrast in material properties represents a stringent test of a model's ability to correctly predict the effective properties of a composite. Again particular attention should be paid to the correlation with the square array predictions obtained from the finite element analyzes. The predictions for the axial Young's modulus (not shown) are the same for all of the models (as expected). The predictions for the effective transverse Young's modulus are given in Fig. 2. The results generated by the ECM and MOC are nearly the same and compare well with the predictions of N–S over the entire range of fiber volume fractions where the N–S results were generated. At higher fiber volume fractions the MOC and ECM predictions converge to the results generated by B–H although the differences at lower volume fractions are appreciable. Consideration of the predictions for the axial Poisson's ratio, Fig. 3, shows that both the MOC and ECM provide accurate predictions with the ECM results being in slightly better agreement with the N–S results. The results for the transverse Poisson's ratio, Fig. 4, exhibit noticeable differences between all of the models. Comparing the MOC and ECM values to the N–S square array predictions indicates that, in general, the ECM more accurately predicts this bulk property than does the MOC. At the lowest volume fractions, 0.125 and 0.25, the ECM and MOC results are not bounded by either of the N–S results although at zero volume fraction (pure epoxy matrix) all models do correctly predict the appropriate value for the Poisson's ratio. At volume fractions above 0.25, the ECM and MOC predictions are bounded by the N–S results. As the volume fraction increases both the ECM and MOC results converge towards each other and the N–S square array results. At a volume fraction of 0.875 the MOC and ECM results exhibit no significant differences. At all volume fractions the B–H results lie below the other model predictions.

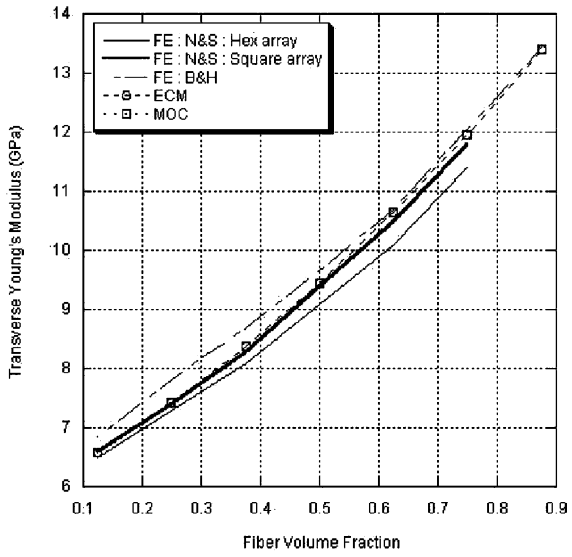

Fig. 2. The effective transverse Young's modulus as a function of fiber volume fraction for a Gr/Ep system.

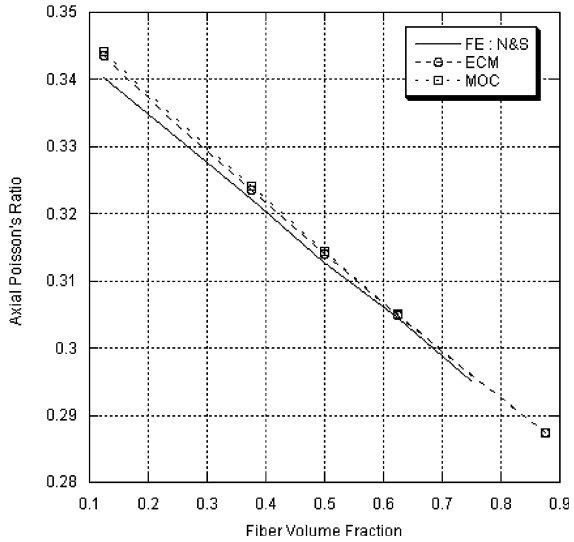

Fig. 3. The effective axial Poisson's ratio as a function of fiber volume fraction for a Gr/Ep system.

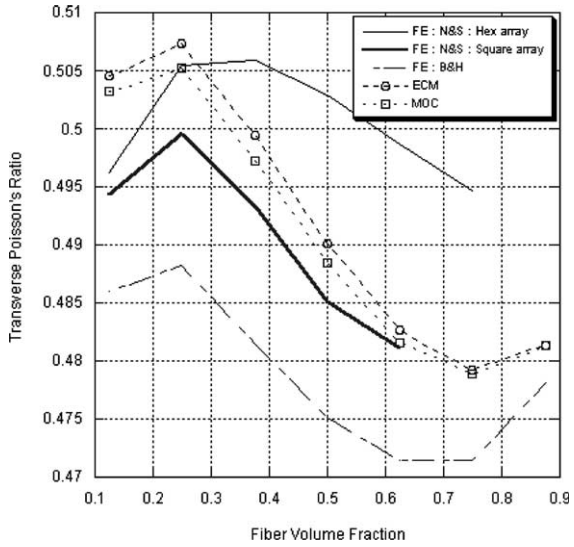

Fig. 4. The effective transverse Poisson's ratio as a function of fiber volume fraction for a Gr/Ep system.

The results for the axial shear modulus are given in Fig. 5. At lower volume fractions the ECM calculations coincide with the N–S FE results. As the volume fraction increases the ECM results more closely approach the hexagonal array predictions of N–S. The MOC results fall below the ECM predictions at all but the highest volume fraction where its predictions coincide with the ECM predictions. Finally, the correlations for the effective transverse shear modulus are considered, Fig. 6. Again, the ECM and N–S square array values are in excellent agreement through the entire range of volume fractions for which the N–S data has been given. The MOC results again fall below the predictions obtained from the other models for all but the highest volume fractions where the ECM and MOC data coincide.

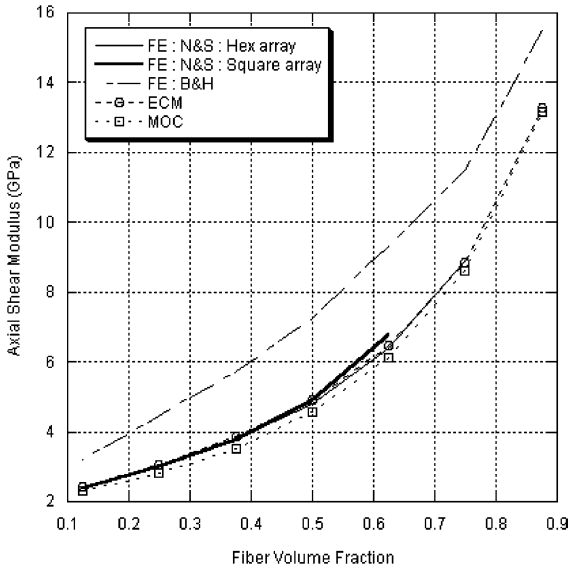

Fig. 5. The effective axial shear modulus as a function of fiber volume fraction for a Gr/Ep system.

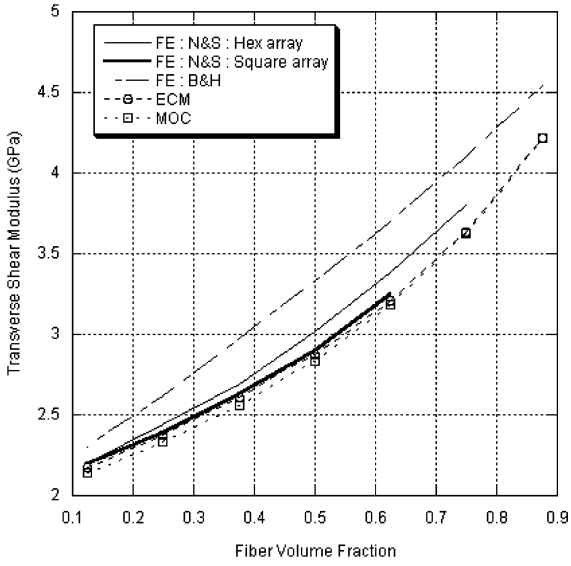

Fig. 6. The effective transverse shear modulus as a function of fiber volume fraction for a Gr/Ep system.

Next, the ECM's (and in some cases the MOC) predictions for both the bulk response and the local fields are compared to the Green's function based analyzes of Walker et al. (1993) that considered the response of void/Cu and W/Cu composites. The model presented by Walker et al. (1993) is based on a singular integral equation approach using Green's functions or (equivalently) Fourier series. The resulting theoretical analysis represents an exact solution to the governing differential equations of a heterogeneous material. The implementation of the solution equations, however, must be carried out using an approximate discretized volume approach. Walker et al. considered the convergence behavior of the Green's function based analysis

by considering increasingly greater numbers of unit cells and discretizations of the unit cells. The Green's function predictions used in the following comparisons where considered by Walker et al. to represent the converged solution and are based on calculations using 25 unit cells of the type shown in Fig. 1. Since the Green's function theory is based on an exact analysis of the governing continuum equations the converged results can be considered to accurately represent the local field solution as well as the bulk composite response. Each of these unit cells was subdivided into 49 subvolumes for the three lowest fiber volume fractions and 225 subvolumes for the highest fiber volume fraction. Thus, the model calculations are based on the use of either 1225 or 5625 subelements which have six unknowns per subelement. It is noted that largest number of unknowns in the ECM (the fifth order version) is 48. Additional details of the modeling approach are given by Nemat-Nasser and Hori (1993). In the following discussion this model will be referred to as the G–F modeling approach.

The results for this part of the discussion have been generated by modeling square inclusions. The use of square inclusions represents a stringent test of a theory's ability to correctly model the local and global behavior of a composite due to the presence of the strong gradients in the local fields induced by the presence of corners. The constituent properties are given in Table 5. The first set of results to be considered are the predictions for the effective transverse Young's modulus for the void/Cu composite at void volume fractions of 0.0204, 0.1837, 0.5102, and 0.7511, Table 6. Both third and fifth order ECM results as well as the corresponding MOC results are presented. Both the MOC and 3rd order ECM results under predict the effective behavior with the largest difference (about 8%) occurring at the lowest volume fraction (0.0204). As the volume fraction of the voids increases both models provide more accurate predictions for the effective behavior (with differences of less than 3%). Consideration of the fifth order ECM results indicates that this model provides better predictions for the effective response with differences of no more than 3%. If instead of a void the inclusion is considered to be tungsten, Table 7, then both versions of the ECM as well as the MOC model provide accurate estimates for the effective transverse Young's modulus with the fifth order ECM providing the most accurate values.

Now the ability of the ECM to predict the variations in the local fields is considered by comparing the ECM results for the local transverse stress to the corresponding G–F results for the W/Cu composite discussed above. The results are obtained by applying a transverse stress of 1000 MPa to the composite in the case of the G–F model. This bulk loading state corresponds to the physical problem of a transverse, uniaxial tension test typically used to characterize the transverse behavior of composite materials. To generated the ECM results an equivalent bulk strain field is applied. This bulk strain field is calculated using

Table 5
Properties for tungsten and copper constituents (Walker et al., 1993)

Material	E (GPa)	v	G (GPa)
Tungsten	395.0	0.28	154.3
Copper	127.0	0.34	47.39

Table 6
Transverse Young's modulus (GPa) for a voided copper composite as a function of the void volume fraction (Walker et al., 1993)

Model	$c_v = 0.0204$	$c_v = 0.1837$	$c_v = 0.5102$	$c_v = 0.7511$
G–F	120.63	83.50	40.48	18.40
MOC	110.20	75.27	38.22	17.99
Third order ECM	110.20	75.38	38.23	17.99
Fifth order ECM	118.90	80.97	39.64	18.20

Table 7
Transverse Young's modulus (GPa) for a W/Cu composite as a function of the void volume fraction (Walker et al., 1993)

Model	$c_f = 0.0204$	$c_f = 0.1837$	$c_f = 0.5102$	$c_f = 0.7511$
G–F	129.87	156.18	229.09	300.70
MOC	129.50	154.40	226.20	299.00
Third order ECM	129.50	154.60	226.60	299.10
Fifth order ECM	129.80	156.50	229.50	300.80

the predicted effective properties of the composite obtained from the ECM. Results from both the third and fifth order version of the ECM are examined. Since the ECM approach provides pointwise variations in the local fields within a subcell, local averaging of the spatial fields in the ECM subcells was used to generate the results for the subelement regions modeled by the G–F model. The predicted local fields obtained from the G–F model and the third and fifth order ECM are given in Figs. 7–10. The first number in a subregion is the value obtained from the G–F analysis, the second is the prediction from the third order ECM, and the last value is the fifth order ECM prediction. The heavy solid lines are the boundaries of the unit cell, the heavy dashed lines represent the boundaries of the subcells, and the light dashed lines represent the subregions within each subcell used in the G–F calculations. All errors discussed below are referenced to the G–F solution.

The general trends in the distributions of the local fields predicted by the different versions of the ECM are in good agreement with the G–F model results, Figs. 7–10. In particular, the required symmetries with respect to the fiber centerlines are correctly predicted by both versions of the ECM. The broad trends in the spatial variations, i.e. magnitudes increasing/decreasing with changing position, are, in general, correctly predicted by both versions of the ECM with the fifth order theory providing the most accurate results. In particular, the third order ECM correctly predicts the locations of the maximum and minimum values in the distributions for the volume fractions of 0.1837 and 0.5102, as well as correctly positioning the minimum value of the local field at the 0.7511 volume fraction. The fifth order ECM predicts the locations of the minimum and maximum values in the local fields for all volume fractions except for the 0.7511 volume

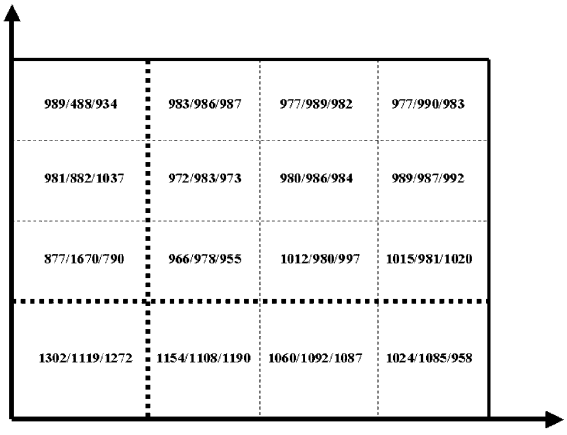

Fig. 7. The local stress field predictions from the Green's function analysis and both versions of the ECM for a W/Cu composite with a fiber volume of 0.0204. The heavy dashed lines represent the boundaries of the subcells in the ECM model. The fine dashed lines represent the boundaries of the computational cells used in the Green's function analysis. With regard to the ordering of the predictions, the first number in each triplet in each GF computational cell is the Green's function prediction, the second number is the third order ECM prediction, and the last number is the fifth order ECM prediction.

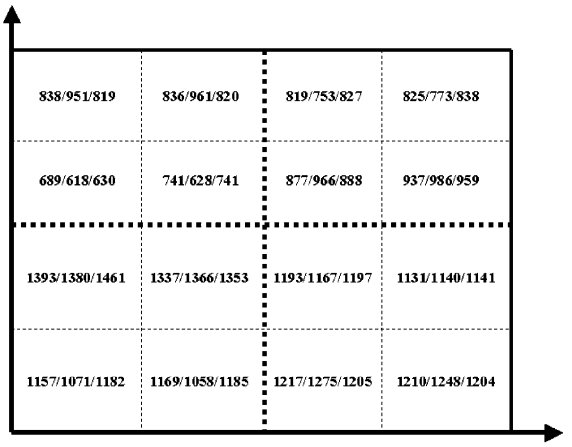

Fig. 8. The local stress field predictions from the Green's function analysis and both versions of the ECM for a W/Cu composite with a fiber volume of 0.1837. The heavy dashed lines represent the boundaries of the subcells in the ECM model. The fine dashed lines represent the boundaries of the computational cells used in the Green's function analysis. With regard to the ordering of the predictions, the first number in each triplet in each GF computational cell is the Green's function prediction, the second number is the third order ECM prediction, and the last number is the fifth order ECM prediction.

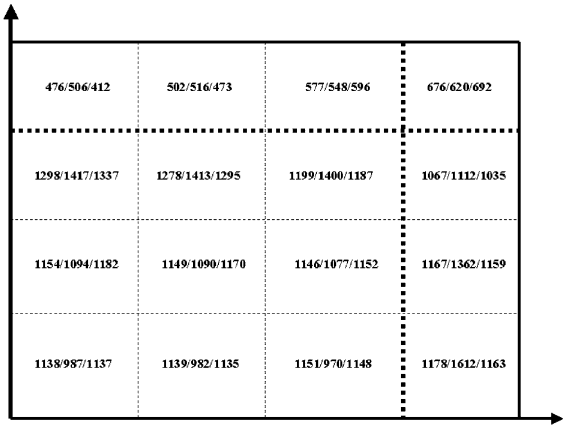

Fig. 9. The local stress field predictions from the Green's function analysis and both versions of the ECM for a W/Cu composite with a fiber volume of 0.5102. The heavy dashed lines represent the boundaries of the subcells in the ECM model. The fine dashed lines represent the boundaries of the computational cells used in the Green's function analysis. With regard to the ordering of the predictions, the first number in each triplet in each GF computational cell is the Green's function prediction, the second number is the third order ECM prediction, and the last number is the fifth order ECM prediction.

fraction were it does not correctly predict the location of the maximum value. Since the differences in the predictions from the G–F and fifth order ECM at this location only differ by 2.97% this exception is relatively insignificant.

Considering the correlations between the third order ECM and the G–F model for the spatial variations in the local fields shows that fairly large errors (up to 90% for a volume fraction of 0.0204 and up to 40% for a volume fraction of 0.7511) occur in the ECM results for the lowest and highest volume fractions while at the volume fractions of 0.1837 and 0.5102 the agreement is, in general, good (with errors of less than 17%). The overall errors in the predicted local fields are, in general, substantially less than the

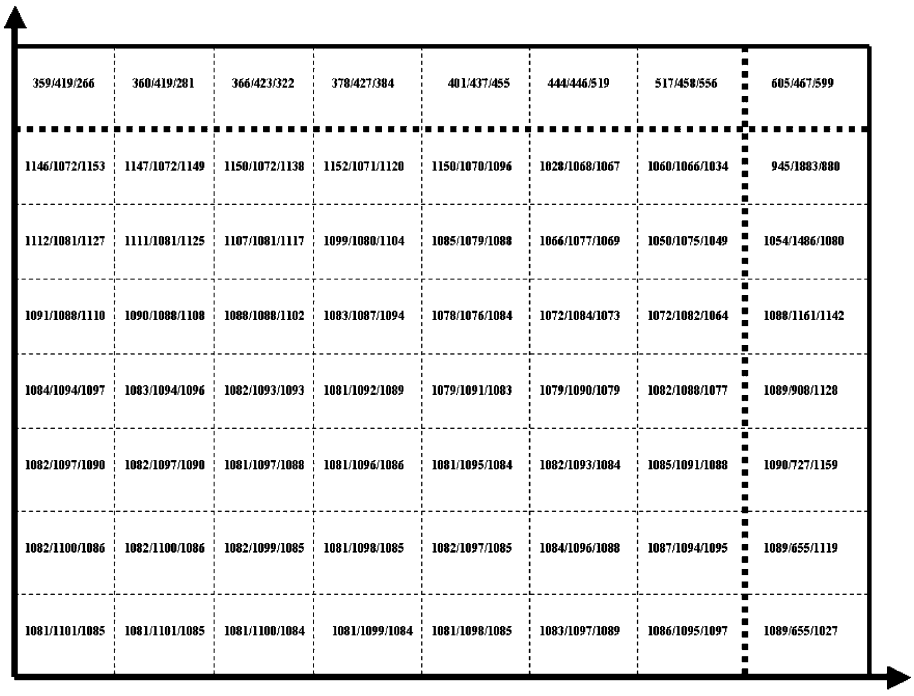

Fig. 10. The local stress field predictions from the Green's function analysis and both versions of the ECM for a W/Cu composite with a fiber volume of 0.7511. The heavy dashed lines represent the boundaries of the subcells in the ECM model. The fine dashed lines represent the boundaries of the computational cells used in the Green's function analysis. With regard to the ordering of the predictions, the first number in each triplet in each GF computational cell is the Green's function prediction, the second number is the third order ECM prediction, and the last number is the fifth order ECM prediction.

maximum errors for the different cases. As might be expected, increasing the size of the region over which the local fields (particularly in the case of 0.0204 volume fraction) are averaged results in better agreement in the predictions obtained from the two models. Consideration of the fifth order ECM results indicates that at all volume fractions the results are in better agreement with G–F predictions than the third order ECM results. At a volume fraction of 0.0204, 0.1837, 0.5102, and 0.7511 the maximum error is less than 10%, 8.5%, 6.5%, and 25%, respectively. It is worth noting in the case of the 0.7511 volume fraction the maximum error occurs in the region with the minimum local stress. In general, the errors in the fifth order ECM predictions as compared to the G–F values are much smaller than the quoted maximum errors given above.

Comparing the results for the ECM and the model proposed by Williams and Aboudi (1999) (not shown) indicates that the current approach represents a far more accurate analysis tool than the older model. For example, the maximum error in the predictions for the local stresses in the matrix obtained from the older model is 52.5% while the corresponding error due to the third order ECM is 6.32%.

6. Summary and conclusion

A new homogenization theory utilizing a higher order, 2D, elasticity based cell analysis has been presented. The ECM model is based on a simplification of the microstructure that represents the fiber as a single region (subcell) surrounded by three matrix regions (subcells). This microstructural simplification is

the same as that used by the original MOC theory. The solution approach is based on truncated eigenfunction expansions up to fifth (cumulative) order for the displacement field. The theory directly and exactly satisfies the strong (pointwise) form of all of the governing equations for geometrically linear continuum mechanics up through the order of the expansions. The analysis is carried out independently of any constitutive models for the materials in the sense that the governing equations are appropriate for any constitutive theory. The proposed fifth order theory is specialized to a third order theory and both the fifth and third order theories collapse to a first order theory that is consistent with the original MOC analysis proposed by Aboudi (1991). In fact, the current formulation shows that the original MOC model can be reinterpreted as a lowest order elasticity solution rather than the weak formulation originally suggested by Aboudi.

The proposed theory has been validated/verified through comparisons with results from the open literature. In particular, the effective properties predicted by the ECM have been compared to a number of different finite element simulations for a number of different material systems with significant contrast in material properties for the phases and for a wide variety of fiber volume fractions. In all cases the theory was shown to provide accurate predictions for the bulk response characteristics of continuous fiber composite systems. It was also shown that ECM provides better estimates for the shear moduli than are obtained from the MOC model over a broad range of inclusion volume fractions. At the very highest volume fractions the predictions for the ECM and MOC model tend to coincide.

The predictions for both the global response and the local fields obtained from the proposed theory were also compared to the results generated using a Green's function analysis. The bulk properties predicted by both approaches for both void/Cu and W/Cu composites were seen to be in good agreement. It was noted that increasing the order of the expansion functions (from third to fifth order) in the ECM improved the agreement between the ECM and Green's function predictions. The implication is that the higher order theory more accurately models the influence of a square inclusion (as is consistent with expectations). This improvement was most noticeable in the case of the composite composed of periodic voids. Comparison of the local fields at different volume fractions generated by both the ECM and Green's function analysis shows that the both the third and fifth order ECM were capable of accurately predicting these local phenomena. In particular, both versions of the ECM provide good estimates for the trends in the local fields as well as the magnitudes of these fields. The accuracy of the predictions for the local behavior improves as the order of the ECM is increased.

In summary, the ability of the proposed ECM to accurately predict both the bulk behavior as well as the local fields shows that the theory represents a viable tool for modeling the behavior of fibrous composites.

One of the most important contributions of the current work is that it represents the necessary theoretical foundations for the development of exact homogenization solutions of generalized, two-dimensional microstructures. While the proposed model has been shown to provide good estimates for the local response it can certainly be expected that higher order expansions and/or greater degrees of refinement in discretizing the material microstructure will lead to improved accuracy for predicting the local fields. The extension of the theory to both higher order approximations and arbitrary microstructural discretizations will be carried out in future work.

Appendix A

This appendix contains the expanded forms of the various field expansions, the definitions for the fluctuating strain effects (the $\mu_{ij(mn)}$), and examples of the mathematical manipulations associated with obtaining the continuity equations and the equilibrium equations given in the main body of the paper. Note that in the following discussion when the superscripts (β,γ) have been dropped it is to be understood that the expression applies to all subcells.

The expanded form of the displacement within a subcell for the fifth order theory is given by

$$u_i = \overline{\epsilon}_{ij}x_j + P_{(01)}V_{i(01)} + P_{(10)}V_{i(10)} + P_{(03)}V_{i(03)} + P_{(12)}V_{i(12)} + P_{(21)}V_{i(21)} + P_{(30)}V_{i(30)} + P_{(05)}V_{i(05)} + P_{(14)}V_{i(14)} + P_{(23)}V_{i(23)} + P_{(32)}V_{i(32)} + P_{(41)}V_{i(41)} + P_{(50)}V_{i(50)} \tag{A.1}$$

The corresponding subcell strain field is

$$\epsilon_{ij} = P_{(00)}\left(\overline{\epsilon}_{ij} + \mu_{ij(00)}\right) + P_{(02)}\mu_{ij(02)} + P_{(11)}\mu_{ij(11)} + P_{(20)}\mu_{ij(20)} + P_{(04)}\mu_{ij(04)} + P_{(13)}\mu_{ij(13)} + P_{(22)}\mu_{ij(22)} + P_{(31)}\mu_{ij(31)} + P_{(40)}\mu_{ij(40)} \tag{A.2}$$

and the associated subcell stress field is

$$\sigma_{ij} = P_{(00)}\sigma_{ij(00)} + P_{(02)}\sigma_{ij(02)} + P_{(11)}\sigma_{ij(11)} + P_{(20)}\sigma_{ij(20)} + P_{(04)}\sigma_{ij(04)} + P_{(13)}\sigma_{ij(13)} + P_{(22)}\sigma_{ij(22)} + P_{(31)}\sigma_{ij(31)} + P_{(40)}\sigma_{ij(40)} \tag{A.3}$$

The particular expressions for the fifth order fluctuating strains in the subcells are

$$\mu_{11(00)} = 0$$

$$\mu_{22(00)} = V_{2(10)} + \left(\frac{h_\beta}{2}\right)^2 V_{2(30)} + \left(\frac{h_\beta}{2}\right)^4 V_{2(50)}$$

$$\mu_{22(02)} = V_{2(12)} + 3\left(\frac{h_\beta}{2}\right)^2 V_{2(32)}$$

$$\mu_{22(11)} = 3V_{2(21)} + 3\left(\frac{h_\beta}{2}\right)^2 V_{2(41)}$$

$$\mu_{22(20)} = 5V_{2(30)} + 5\left(\frac{h_\beta}{2}\right)^2 V_{2(50)}$$

$$\mu_{22(04)} = 0$$

$$\mu_{22(13)} = 3V_{2(23)}$$

$$\mu_{22(22)} = 5V_{2(32)}$$

$$\mu_{22(31)} = 7V_{2(41)}$$

$$\mu_{22(40)} = 9V_{2(50)}$$

$$\mu_{33(00)} = V_{3(01)} + \left(\frac{l_\gamma}{2}\right)^2 V_{3(03)} + \left(\frac{l_\beta}{2}\right)^4 V_{3(05)}$$

$$\mu_{33(02)} = 5V_{3(03)} + 5\left(\frac{l_\gamma}{2}\right)^2 V_{3(05)}$$

$$\mu_{33(11)} = 3V_{3(12)} + 3\left(\frac{l_\gamma}{2}\right)^2 V_{3(14)}$$

$$\mu_{33(20)} = V_{3(21)} + \left(\frac{l_\gamma}{2}\right)^2 V_{3(23)}$$

$$\mu_{33(04)} = 9V_{3(05)}$$

$$\mu_{33(13)} = 7V_{3(14)}$$

$$\mu_{33(22)} = 5V_{3(23)}$$

$$\mu_{33(31)} = 3V_{3(32)}$$

$$\mu_{33(40)} = 0$$

$$\mu_{23(00)} = \frac{1}{2}\left(V_{2(01)} + \left(\frac{l_\gamma}{2}\right)^2 V_{2(03)} + \left(\frac{l_\gamma}{2}\right)^4 V_{2(05)} + V_{3(10)} + \left(\frac{h_\beta}{2}\right)^2 V_{3(30)} + \left(\frac{h_\beta}{2}\right)^4 V_{3(50)}\right)$$

$$\mu_{23(02)} = \frac{1}{2}\left(5V_{2(03)} + 5\left(\frac{l_\gamma}{2}\right)^2 V_{2(05)} + V_{3(12)} + \left(\frac{h_\beta}{2}\right)^2 V_{3(32)}\right)$$

$$\mu_{23(11)} = \frac{1}{2}\left(3V_{2(12)} + 3\left(\frac{l_\gamma}{2}\right)^2 V_{2(14)} + 3V_{3(21)} + 3\left(\frac{h_\beta}{2}\right)^2 V_{3(41)}\right)$$

$$\mu_{23(20)} = \frac{1}{2}\left(V_{2(21)} + \left(\frac{l_\gamma}{2}\right)^2 V_{2(23)} + 5V_{3(30)} + 5\left(\frac{h_\beta}{2}\right)^2 V_{3(50)}\right)$$

$$\mu_{23(04)} = \frac{1}{2}\left(9V_{2(05)} + V_{3(14)}\right)$$

$$\mu_{23(13)} = \frac{1}{2}\left(7V_{2(14)} + 3V_{3(23)}\right)$$

$$\mu_{23(22)} = \frac{1}{2}\left(5V_{2(23)} + 5V_{3(32)}\right)$$

$$\mu_{23(31)} = \frac{1}{2}\left(3V_{2(32)} + 7V_{3(41)}\right)$$

$$\mu_{23(40)} = \frac{1}{2}\left(V_{2(41)} + 9V_{3(50)}\right)$$

$$\mu_{13(00)} = \frac{1}{2}\left(V_{1(01)} + \left(\frac{l_\gamma}{2}\right)^2 V_{1(03)} + \left(\frac{l_\gamma}{2}\right)^4 V_{1(05)}\right)$$

$$\mu_{13(02)} = \frac{1}{2}\left(5V_{1(03)} + \left(\frac{l_\gamma}{2}\right)^2 V_{1(05)}\right)$$

$$\mu_{13(11)} = \frac{1}{2}\left(3V_{1(12)} + 3\left(\frac{l_\gamma}{2}\right)^2 V_{1(14)}\right)$$

$$\mu_{13(20)} = \frac{1}{2}\left(V_{1(21)} + \left(\frac{l_\gamma}{2}\right)^2 V_{1(23)}\right)$$

$$\mu_{13(04)} = \frac{9}{2} V_{1(05)}$$
$$\mu_{13(13)} = \frac{7}{2} V_{1(14)}$$
$$\mu_{13(22)} = \frac{5}{2} V_{1(23)}$$
$$\mu_{13(31)} = \frac{3}{2} V_{1(32)}$$
$$\mu_{13(40)} = \frac{1}{2} V_{1(41)}$$

$$\mu_{12(00)} = \frac{1}{2}\left(V_{1(10)} + \left(\frac{h_\beta}{2}\right)^2 V_{1(30)} + \left(\frac{h_\beta}{2}\right)^4 V_{1(50)} \right)$$
$$\mu_{12(02)} = \frac{1}{2}\left(V_{1(12)} + \left(\frac{h_\beta}{2}\right)^2 V_{1(32)} \right)$$
$$\mu_{12(11)} = \frac{1}{2}\left(3V_{1(21)} + 3\left(\frac{h_\beta}{2}\right)^2 V_{1(41)} \right)$$
$$\mu_{12(20)} = \frac{1}{2}\left(5V_{1(30)} + 5\left(\frac{h_\beta}{2}\right)^2 V_{1(50)} \right)$$

$$\mu_{12(04)} = \frac{1}{2} V_{1(14)}$$
$$\mu_{12(13)} = \frac{3}{2} V_{1(23)}$$
$$\mu_{12(22)} = \frac{5}{2} V_{1(32)}$$
$$\mu_{12(31)} = \frac{7}{2} V_{1(41)}$$
$$\mu_{12(40)} = \frac{9}{2} V_{1(50)}$$

The appropriate forms for the Legendre polynomials up through fifth order are

$$P_{(0)} = 1$$
$$P_{(1)} = x$$
$$P_{(2)} = \frac{1}{2}\left(3x^2 - \frac{d^2}{4} \right)$$
$$P_{(3)} = \frac{1}{2}\left(5x^3 - 3\frac{d^2}{4} x \right)$$
$$P_{(4)} = \frac{1}{8}\left(35x^4 - 30\frac{d^2}{4} x^2 + 3\frac{d^4}{16} \right)$$
$$P_{(5)} = \frac{1}{8}\left(63x^5 - 70\frac{d^2}{4} x^3 + 15\frac{d^4}{16} x \right)$$

where d is the subcell dimension along a given direction.

The details of the manipulations associated with the equilibrium equations are given next. Substituting the stress expansion, Eq. (2.4) or (A.3), into the equilibrium equation gives

$$\begin{aligned}
&\left(3\sigma^{(\beta,\gamma)}_{i2(20)}+\sigma^{(\beta,\gamma)}_{i3(11)}+3\left(\frac{h_\beta}{2}\right)^2\sigma^{(\beta,\gamma)}_{i2(40)}+\left(\frac{l_\gamma}{2}\right)^2\sigma^{(\beta,\gamma)}_{i3(13)}\right)P_{(10)}\\
&\quad+\left(\sigma^{(\beta,\gamma)}_{i2(11)}+3\sigma^{(\beta,\gamma)}_{i3(02)}+\left(\frac{h_\beta}{2}\right)^2\sigma^{(\beta,\gamma)}_{i2(31)}+3\left(\frac{l_\gamma}{2}\right)^2\sigma^{(\beta,\gamma)}_{i3(04)}\right)P_{(01)}+\left(7\sigma^{(\beta,\gamma)}_{i2(40)}+\sigma^{(\beta,\gamma)}_{i3(31)}\right)P_{(30)}\\
&\quad+\left(5\sigma^{(\beta,\gamma)}_{i2(31)}+3\sigma^{(\beta,\gamma)}_{i3(22)}\right)P_{(21)}\left(3\sigma^{(\beta,\gamma)}_{i2(22)}+5\sigma^{(\beta,\gamma)}_{i3(13)}\right)P_{(12)}+\left(7\sigma^{(\beta,\gamma)}_{i2(40)}+\sigma^{(\beta,\gamma)}_{i3(31)}\right)P_{(03)}=0
\end{aligned}\tag{A.4}$$

As in standard eigenfunction formulations, the appropriate forms for the equilibrium equations are obtained by multiplying Eq. (A.4) by the various potential orders of the spatial variations, i.e. the various $P_{(nr)}$, integrating the result over the volume of that subcell, and using the fact that the expansion polynomials are orthogonal. The resulting equations are identically Eqs. (2.5)–(2.10). As noted in the text the orthogonalization process is equivalent to simply equating each set of terms of different order in Eq. (A.4) to zero.

An example of the decoupling process for the continuity equations is presented below. While the particular example is for a given order of the displacement continuity equations the concepts behind the manipulations can be applied to any of the different continuity equations. Consider the zeroth order displacement continuity relations for a fifth order theory in the x_2-direction *assuming that all terms in the expansions are present*. For the interface within the unit cell the appropriate displacement continuity relation in this situation is given by

$$\begin{aligned}
&\frac{h_1}{2}V^{(1,\gamma)}_{i(10)}+\left(\frac{h_1}{2}\right)^2V^{(1,\gamma)}_{i(2)}+\left(\frac{h_1}{2}\right)^3V^{(1,\gamma)}_{i(30)}+\left(\frac{h_1}{2}\right)^4V^{(1,\gamma)}_{i(30)}+\left(\frac{h_1}{2}\right)^5V^{(1,\gamma)}_{i(50)}\\
&\quad=-\frac{h_2}{2}V^{(2,\gamma)}_{i(10)}+\left(\frac{h_2}{2}\right)^2V^{(2,\gamma)}_{i(20)}-\left(\frac{h_2}{2}\right)^3V^{(2,\gamma)}_{i(30)}+\left(\frac{h_2}{2}\right)^4V^{(2,\gamma)}_{i(20)}-\left(\frac{h_2}{2}\right)^5V^{(2,\gamma)}_{i(50)}
\end{aligned}\tag{A.5}$$

For the interface between unit cells the appropriate form for the displacement continuity relation is

$$\begin{aligned}
&-\frac{h_1}{2}V^{(1,\gamma)}_{i(10)}+\left(\frac{h_1}{2}\right)^2V^{(1,\gamma)}_{i(2)}-\left(\frac{h_1}{2}\right)^3V^{(1,\gamma)}_{i(30)}+\left(\frac{h_1}{2}\right)^4V^{(1,\gamma)}_{i(30)}-\left(\frac{h_1}{2}\right)^5V^{(1,\gamma)}_{i(50)}\\
&\quad=\frac{h_2}{2}V^{(2,\gamma)}_{i(10)}+\left(\frac{h_2}{2}\right)^2V^{(2,\gamma)}_{i(20)}+\left(\frac{h_2}{2}\right)^3V^{(2,\gamma)}_{i(30)}+\left(\frac{h_2}{2}\right)^4V^{(2,\gamma)}_{i(20)}+\left(\frac{h_2}{2}\right)^5V^{(2,\gamma)}_{i(50)}
\end{aligned}\tag{A.6}$$

Adding Eqs. (A.5) and (A.6) gives

$$\left(\frac{h_1}{2}\right)^2V^{(1,\gamma)}_{i(2)}+\left(\frac{h_1}{2}\right)^4V^{(1,\gamma)}_{i(30)}=\left(\frac{h_2}{2}\right)^2V^{(2,\gamma)}_{i(20)}+\left(\frac{h_2}{2}\right)^4V^{(2,\gamma)}_{i(20)}\tag{A.7}$$

Subtracting Eqs. (A.5) and (A.6) gives Eq. (2.11). From these manipulations it is obvious that the different order effects in the continuity equations can be decoupled.

References

Aboudi, J., 1991. Mechanics of Composite Materials: A Unified Micromechanics Approach. Elsevier, New York, NY.

Aboudi, J., 1996. Micromechanical analysis of composites by the method of cells—update. Appl. Mech. Rev. 49, 127–139.

Aboudi, J., Pindera, M.-J., Arnold, S.M., 2001. Linear thermo-elastic higher-order theory for periodic multiphase materials. J. Appl. Mech. 68, 697–707.

Bennett, J.G., Haberman, K.S., 1996. An alternate unified approach to the micromechanical analysis of composite materials. J. Compos. Mater. 30, 1732–1747.

Bensoussan, A., Lions, J.L., Papanicolaou, G., 1978. Asymptotic Analysis for Periodic Structures. North-Holland, New York, NY.

Benveniste, Y., 1987. A new approach to the application of Mori–Tanaka's theory in composite materials. Mech. Mater. 6, 147–157.

Christensen, R.M., 1979. Mechanics of Composite Materials. Wiley and Sons, New York, NY.

Eshelby, J.D., 1957. The determination of the elastic field of an ellipsoidal inclusion, and related problems. Proc. R. Soc. Lond. A A241, 376–396.

Gilat, R., 1998. On the variational consistency of the higher-order-shear- deformation plate equations derived from the 3-D differential equations of motion. Compos. Struct. 41, 285–287.

Lissenden, C.J., Herakovich, C.T., 1992. Comparison of micromechanical models for elastic properties. In: Sadeh, W.Z., Sture, S., Miller, R.J., Denver, C.O, editors. Space 92, Proceeding of the 3rd International Conference on Engineering, Construction, and Operations in Space III. May 31–June 4, pp. 1309–1322.

Nemat-Nasser, S., Hori, M., 1993. Micromechanics: Overall Properties of Heterogeneous Materials. North-Holland, New York, NY.

Noor, A.K., Shah, R.S., 1993. Effective thermoelastic and thermal properties of unidirectional fiber-reinforced composites and their sensitivity coefficients. Compos. Struct. 26, 7–23.

Paley, M., Aboudi, J., 1992. Micromechanical analysis of composites by the generalized method of cells. Mech. Mater. 14, 127–139.

Soldatos, K.P., 1995. Generalization of variationally consistent plate theories on the basis of a vectorial formulation. J. Sound Vib. 183, 819–839.

Sun, C.T., Vaidya, R.S., 1996. Prediction of composite properties from a representative volume element. Compos. Sci. Technol. 86, 171–179.

Walker, K.P., Freed, A.D., Jordan, E.H., 1993. Accuracy of the generalized self-consistent method in modelling the elastic behavior of periodic composites properties of unidirectional fiber-reinforced composites and their sensitivity coefficients. Philos. Trans. R. Soc. Lond. A 345, 545–576.

Williams, T.O., Aboudi, J., 1999. A generalized micromechanics model with shear-coupling. Acta Mech. 138, 131–154.

Williams, T.O., Pindera, M.J., 1995. Thermo-mechanical fatigue modeling of advanced metal matrix composites in the presence of microstructural details. Mater. Sci. Eng. A 200, 156–172.

Williams, T.O., Pindera, M.J., 1997. An analytical model for the inelastic longitudinal shear response of metal matrix composites. Int. J. Plasticity 13, 261–289.